Ultraviolet Spectra and Excited States of Formaldehyde

D. C. MOULE* and A. D. WALSH**

Departments of Chemistry, Brock University, St. Catharines, Ontario, Canada, and The University of Dundee, Dundee, Scotland

Received September 14, 1973 (Revised Manuscript Received January 21, 1974)

Contents

I. Introduction

"Mettez une goutte d'éther dans un verre froid . . . , chauffez sur un morceau de fer, ou à la flame d'une bougie, un fil de platine roulé en spiral; plongez ce fil dans le verre, il deviendra resplendissant. Lorsqu'on fait l'expérience de la combustion lente de l'éther dans l'obscurité, on apercoit au-dessus du fil une lumière pâle, phosphorescente." Thus wrote Sir Humphrey Davy in 1817.[1] Immediately following this passage is an account of experiments made by Faraday, at Davy's invitation, to ascertain the nature of the chemical products resulting from these strange phenomena. Perkin's[2] description in 1882 of his observation of the same phenomena makes equally fascinating reading: "When evaporating ether in a shallow vessel on a somewhat strongly heated sand bath, it is always observed that vapour, irritating to the eyes, is formed. Sometime since, when conducting an operation of this kind, in the evening when it is nearly dark, a pale blue flame was seen floating about on the surface of the sand and yet not igniting the ether which was being evaporated. This was repeated several times and always with the same results."

Davy and Perkin were dealing with the same phenomena; viz., the common occurrence of a pale blue light accompanying the gas-phase oxidation of hydrocarbons and their derivatives. The fact that the pale blue flame showed little temperature rise led to its being given the name "cool flame."

Perkin realized that spectroscopic examination might prove whether the faint blue flames emanating from the series of hydrocarbon derivatives were really identical, but the spectroscopes of his day were insufficiently developed to carry out an examination of such a feeble source of light. Spectroscopic examination had to wait until 40 years later when Emeléus[3] succeeded in satisfactorily photographing the spectrum of the cool flame of ether. In his experiments, exposures of 180 hr were necessary to expose properly the photographic plates even with the use of a wide slit and low dispersion. One of the photographs obtained by Emeléus is reproduced in Figure 1A. For nearly 10 years the emitter of the bands still remained unknown. Kondrat'ev[4] suggested that the bands might be due to formaldehyde. Later, Herzberg and Franz[5] and Gradstein[6] photographed the fluorescence spectrum of formaldehyde; and Pearse[7] showed, by direct comparison of the spectrograms, that the position and general distribution of the intensities of the bands in the cool flame spectrum corresponded closely with those of the formaldehyde fluorescence spectrum. Figure 1B is part of the fluorescence spectrum as obtained by Gradstein. Moreover the spectra of the cool flames of acetaldehyde, propionaldehyde, and *n*-hexane were shown to be identical, which made it very probable that the cool flames of ethers, aldehydes, paraffins, and other homologous series are all due to the same emitter, namely, excited formaldehyde.

Throughout its illustrious infancy and precocious childhood, formaldehyde has always displayed certain characteristics which have ensured that it would occupy a prominent position in the field of molecular electronic spectroscopy. The reasons for formaldehyde's uniqueness in this respect are manyfold. Below we briefly list a few reasons why formaldehyde has remained, and probably will remain, a prototype system for the many diverse experiments which involve the near-ultraviolet emission or absorption of light radiation:

(a) Formaldehyde is the simplest compound containing the carbonyl chromophore, and as such is the most commonly used analog in the understanding of its more complex homologs.

(b) The line widths of the electronic transitions in formaldehyde which lie in the near-ultraviolet region are exceedingly narrow and are limited only by the natural Doppler line broadening.

(c) The rotational constants in the electronic states which combine to give the near-ultraviolet spectra are such that the rotational fine structure is only loosely packed into the vibronic band envelopes with the result that the individual *J* lines can be cleanly resolved.

(d) With six degrees of vibrational freedom, the assignment of the vibronic substructure is a nontrivial, although tractable, problem.

(e) The other isotopes of formaldehyde, HDCO and D_2CO, are readily available.

In this review we summarize the results which are available for the ground and higher electronic states of formaldehyde. Emphasis is placed on the molecular structure of H_2CO in its lowest singlet and triplet electronically excited states and, in particular, to those features which pertain to molecular nonplanarity. Several

* Author to whom correspondence should be addressed at Brock University.
** The University of Dundee.

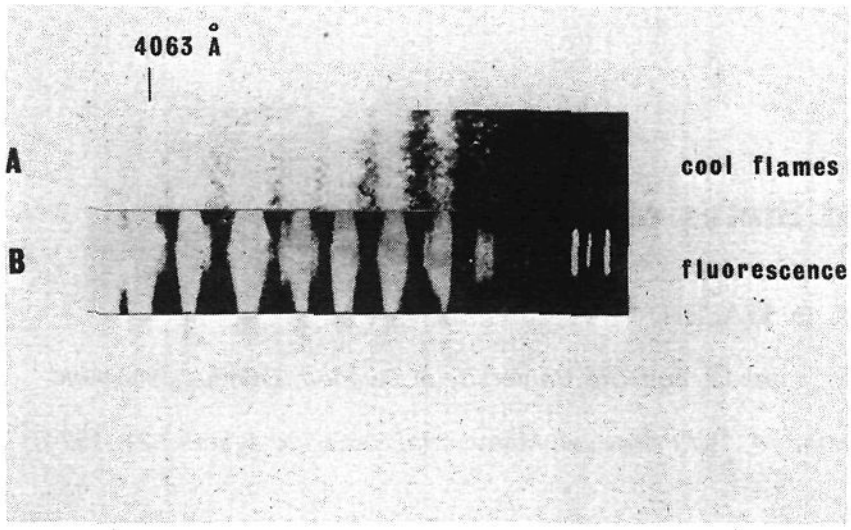

Figure 1. (A) The spectrum of the cool flame of diethyl ether as photographed by Emeléus.[3] (B) Part of the fluorescence spectrum of formaldehyde as obtained by Gradstein.[6]

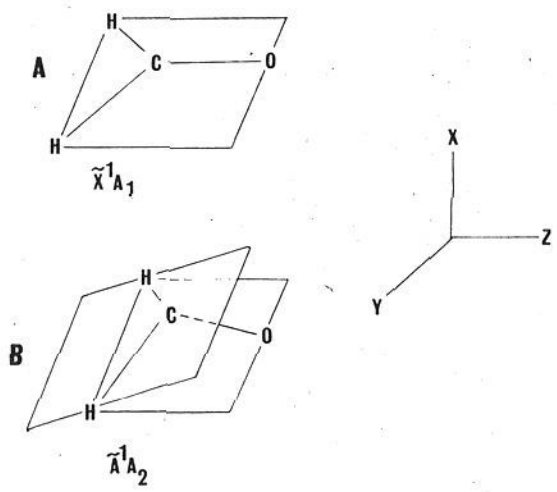

Figure 2. The geometry of formaldehyde in its two lowest singlet states: (A) Structure of the $\tilde{X}^1A_1$ ground electronic state; (B) the $\tilde{A}^1A_2(n,\pi^*)$ state.

figures of H_2CO, HDCO, and D_2CO in the vacuum region are given for the first time along with a new interpretation of the vibronic structures of the 1750- and 1559-Å systems.

II. Electronic States of Formaldehyde

A. Intravalence States

The molecular orbitals of planar formaldehyde can be classified according to their behavior under the symmetry operations of the point group, C_{2v}, for which the character table is given in Table I. As a result of different choices for the Cartesian coordinates by different authors, some ambiguity in the labels of the B_1 and B_2 irreducible representations exists in the literature. For molecules like H_2CO, the recommendation,[8] by the Joint Commission on Spectroscopy of the IAU and the IUPAC, is that the x axis be taken perpendicular to the molecular plane and the z axis as that through the carbon and oxygen atoms. Figure 2 shows the coordinate axis system and the geometry of formaldehyde in its two lowest singlet states.

Simple molecular orbital wave functions for H_2CO may be obtained from a linear combination of atomic 1s(H), 1s(O), 2s(O), $2p_x$(O), $2p_y$(O), $2p_z$(O), 1s(C), 2s(C), $2p_x$(C), $2p_y$(C), and $2p_z$(C) wave functions which satisfy the symmetry requirements of the C_{2v} point group. The s and p_z atomic orbitals on the carbon and oxygen centers transform as translations along the z axis under the operations of the C_{2v} group, and are classified as species a_1. The p_x and p_y AO's transform as x and y and are classified respectively as b_1 and b_2. The MO's of lowest energy which are obtained from the LCAO–MO scheme are a pair labeled $a_1$1s(C) and $a_1$1s(O). These do not contribute to the valence structure and may be regarded as nonbonding orbitals on the carbon and oxygen centers. A MO which bears the description $a_1\sigma$(CO) follows the 1s(C) and 1s(O) orbitals in energy and is formed from the in-phase overlap of the 2s and $2p_z$ AO's of carbon and oxygen. Following this comes a pair of group orbitals $a_1\sigma$(CH) and $b_2\sigma$(CH) which result from the in-plane symmetric and antisymmetric combinations of the 1s(H) AO's of the two hydrogens. The remaining one-electron energy levels of planar formaldehyde and the possible one-electron intravalence transitions are shown in Figure 3, where the small diagrams indicate roughly the charge distributions and the shapes of the molecular orbitals. The orbital labeled $a_1\sigma$n(CO) may be considered to be constructed as a 2s(O)–$2p_z$(O) hybrid MO on the oxygen and is referred to as either a σ(CO) bonding orbital or as a second nonbonding orbital n(CO). Hence our use of the notation $a_1\sigma$n(CO) which represents a combination of the two descriptions. Slightly above this lies the $b_1\pi$(CO) orbital which is formed from the in-phase overlap of the $2p_x$(C) and $2p_x$(O) AO's. This is the orbital which is usually referred to as the π bond. The last stable orbital can be described as a nonbonding b_2n(O) orbital. In its properties, it approximates rather closely to the p_y(O) AO. The antibonding orbitals $b_1\pi^*$(CO), $a_1\sigma^*$(CO), $b_2\sigma^*$(CH), and $a_1\sigma^*$(CH) follow in increasing order.

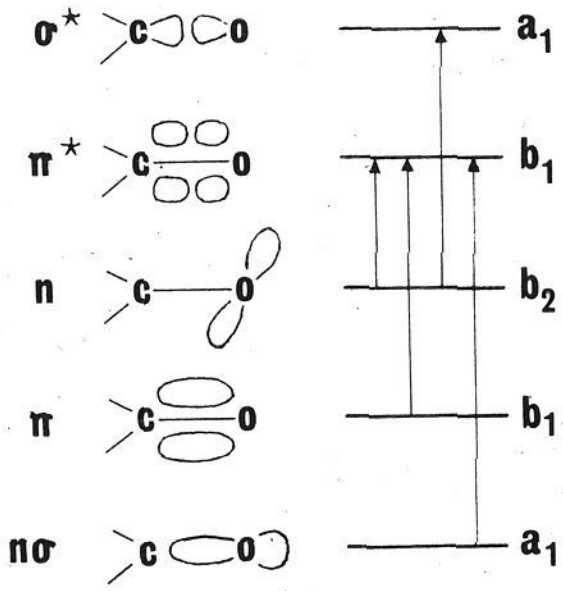

Figure 3. The molecular orbitals and intravalence shell electronic transitions for formaldehyde.

TABLE I. Symmetry Species and Characters for the C_s and C_{2v} Point Groups

C_{2v}	E	C_2	$\sigma(xz)$	$\sigma(yz)$	
A_1	+1	+1	+1	+1	T_z
A_2	+1	+1	−1	−1	
B_1	+1	−1	+1	−1	T_x
B_2	+1	−1	−1	+1	T_y
C_s	E	$\sigma(xz)$			
A′	+1	+1	T_z,T_x		
A″	+1	−1	T_y		

The electronic configuration of the ground state is obtained by placing the 12 valence electrons into the 6 lowest energy levels to fill the manifold of states up to the b_1n(O) level. The electronic configuration of the ground state is therefore

$$(a_1)^2(b_1)^2(b_2)^2 \qquad {}^1A_1$$

Excitation of a single electron from one of the filled $a_1\sigma$n(CO), $b_1\pi$(CO), or b_2n(O) levels to an antibonding $b_1\pi^*$(CO) or $a_1\sigma^*$(CO) level leads to the possible excited states and electronic configurations:

$(a_1)^2(b_1)^2(b_2)(b_1^*)$	$^1A_2, ^3A_2(n,\pi^*)$
$(a_1)^2(b_1)^2(b_2)(a_1^*)$	$^1B_2, ^3B_2(n,\sigma^*)$
$(a_1)^2(b_1)(b_2)^2(b_1^*)$	$^1A_t, ^3A_1(\pi,\pi^*)$
$(a_1)(b_1)^2(b_2)^2(b_1^*)$	$^1B_1, ^3B_t(\sigma n,\pi^*)$
$(a_1)^2(b_1)(b_2)^2(a_1^*)$	$^1B_1, ^3B_t(\pi,\sigma^*)$
$(a_1)(b_1)^2(b_2)^2(a_1^*)$	$^1A_1, ^3A_1(\sigma n,\sigma^*)$

A number of qualitative predictions about the molecular configurations of formaldehyde in its various excited states were successfully made by Walsh,[9] who considered the correlation of the one-electron orbital energies with the changing out-of-plane angle. The primary postulate on which his diagram is based is that a molecular orbital has a lower energy (*i.e.*, contains an electron which is more tightly bound) if, on changing the bond angle at the atomic center, the MO changes from being a p-type orbital to being built from an s-type AO. In Figure 4 the effect of such a distortion in H_2CO is considered. A significant feature of the out-of-plane bending is that the $C_2(z)$ and $\sigma(yz)$ elements of symmetry which are present in the planar form are removed, and thus it becomes necessary to classify the wave functions under the operations of the C_s point group. Those wave functions which belonged to the a_1 and b_1 species in the planar configuration now correlate to the a' representations of the distorted configuration, while those of the a_2 and b_2 species correlate to a''. That is, with a reduction of the OCH and HCH angles, the $a_1\sigma(CO)$ and $b_2\pi(CO)$ one-electron states begin to interact until at $\angle HCH = \angle OCH = 90°$ any distinction between the bonding in the σ and π orbitals is lost.

The variation of the orbital energies as a function of the out-of-plane angle, the correlation diagram, may be derived from the Walsh postulate in a straightforward manner. On the right-hand side of Figure 4 the carbon AO's used in the construction of the $a_1\sigma(CH)$, $b_2\sigma(CH)$, and $a_1\sigma(CO)$ orbitals are sp^2 hybrids; on the left-hand side of the diagram the AO's are pure $p_x(C)$ and $p_y(C)$. Hence the one-electron energies for the three σ orbitals are expected to display an upward shift as the HCH or OCH angle decreases from 120 to 90°. Likewise the $b_1\pi(CO)$ orbital, which is formed from the overlap of the $p_x(O)$ and $p_x(C)$ AO's, is less binding in the bent configuration since these AO's now become involved in the σ-orbital framework. The states which are described as $a_1\sigma(CO)$ and $b_2n(O)$ are only slightly influenced by bending since they may be regarded as nonbonding lone pairs and are expected to show little variation with the out-of-plane angle. The $b_1\pi^*(CO)$ MO, an antibonding combination of the $p_x(O)$ and $p_x(C)$ AO's in the C_{2v} configuration, becomes a nonbonding 2s(C) AO in the C_s configuration. The effect of bending, therefore, is to mix into the $2p_x(C)$ orbital an amount of 2s(C) character which, from the Walsh postulate, results in a lowering of the energy. As it

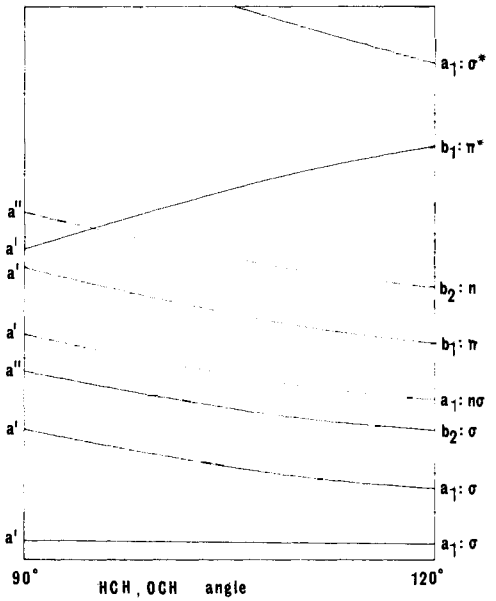

Figure 4. The variation of orbital energy with the HCH or OCH bond angles for formaldehyde.

is only the $b_2\pi^*(CO)$ state which becomes more binding with increasing nonplanar distortion, it follows that only those electronic configurations which occupy the $b_1\pi^*(CO)$ level will display any tendency toward nonplanarity. Of the singlet states, only the $^1A_2(n,\pi^*)$, $^1B_1(\sigma n,\pi^*)$, and $^1A_1(\pi,\pi^*)$ states should be nonplanar. This correlation of one-electron states was confirmed by Brand[10] in 1956 who demonstrated from a detailed analysis of the vibronic substructure of the $\tilde{A}^1A_2(n,\pi^*) \leftarrow \tilde{X}^1A_1$ transition that the nuclear configuration of the upper state was indeed distorted from the molecular plane.

A large number of molecular orbital calculations have been carried out over the past 15 years[11-22] with the aim of predicting the electronic and molecular properties of formaldehyde in its ground and higher electronic states. These calculations have employed the SCF (self-consistent field), CI (configuration interaction) methods, or, in certain instances, combinations of the two. While the bulk of the work has been of a semiempirical nature at various levels of differential overlap (CNDO/2, INDO, CNDO/S, PPP, etc.), a group of detailed *ab initio* calculations have appeared recently in the literature. Table II lists the energies (in eV) which have been calculated for the vertical electronic transitions between the $\tilde{X}^1A_1$ ground state of formaldehyde and the higher singlet and triplet states.

The assignment of the low-intensity 2900-Å system of formaldehyde to the electronic promotion of a $b_2n(O)$ electron which was made in the early 1940's by McMurray and Mulliken[23] is amply confirmed in Table II. The results given in this table are also in agreement about the ordering of the first three excited states: *viz.*, $\tilde{a}^3A_2(n,\pi^*)$,

TABLE II. Comparison of the Calculated Transition Energies (eV) for Formaldehyde

	Semiempirical								*Ab initio*						
Ref	(11)	(12)	(13)	(14)	(15)	(15)	(15)	(16)	(17)	(17)	(18)	(19)	(20)	(21)	(22)
$^1A_2(n,\pi^*)$	4.1	3.5	3.8	3.5	4.6	4.7	3.8	3.6	3.5	3.6	3.4	3.8	3.8		
$^1B_2(n,\sigma^*)$	6.4	8.6			10.3	10.4	8.1	8.1	17	17	10.4				
$^1B_1(\sigma n,\pi^*)$		10.0			8.9	9.1	8.3	9.1	8.6	8.9	8.6	9.4	9.0		8.4
$^1A_1(\pi,\pi^*)$	8.2	9.8	7.4	8.1	11.6	11.8	15.6	9.6	11.2	12.0	12.1	11.3	11.4	9.9	9.8
$^3A_2(n,\pi^*)$	3.7	3.5	3.6	2.7	4.0	4.1	3.5		2.1	2.3	3.0	3.4	3.4		
$^3B_2(n,\sigma^*)$	6.4	8.6			8.0	8.3					10.0				
$^3B_1(\sigma n,\pi^*)$		8.9			7.8	8.1			6.5	7.0	7.6		8.1		
$^3A_1(\pi,\pi^*)$	4.8	5.4	5.1	4.0	5.7	7.2				3.9	5.0	5.7	5.6		

TABLE III. Out-of-Plane Angle and Carbonyl Bond Distances for H_2CO in Various Electronic States[a]

	Out-of-plane angle, deg		R(CO), Å	
	Calcd	Exptl	Calcd	Exptl
$^1A_1$(ground)	0	0	2.35	2.28
$^1A_2(n,\pi^*)$	31.9	26.9	2.64	2.50
$^1B_2(n,\sigma^*)$	0		No min	
$^1B_1(\sigma n,\pi^*)$	7.1		No min	
$^1A_1(\pi,\pi^*)$	0		No min	
$^3A_2(n,\pi^*)$	32.7	35.6	2.60	2.47
$^3B_2(n,\sigma^*)$	0		No min	
$^3B_1(\sigma n,\pi^*)$	25.1		2.80	
$^3A_1(\pi,\pi^*)$	25.9		2.80	

[a] Data taken from Buenker and Peyerimhoff.[15]

$\tilde{A}^1A_2(n,\pi^*)$, and $\tilde{b}^3A_2(\pi,\pi^*)$. The picture for the higher excited states is not so clear, particularly with respect to the location of the $^1B_2(n,\sigma^*)$ level. Of the eight semiempirical calculations quoted in Table II, four place the $^1B_2(n,\sigma^*)$ level between 7.3 and 8.6 eV which makes it the fourth excited state. The *ab initio* calculations, however, place this state at higher energies, *viz.*, 10.4 to 17 eV. The difficulty in obtaining a uniform theoretical prediction for the $^1B_2(n,\sigma^*)$ state may partly arise from a faulty interpretation of the experimental data. In section VI it will be shown in more detail that an absorption system is observed in the vacuum region of formaldehyde which has the correct energy (7.08 eV), oscillator strength (0.038), and polarization (*y*) to be assigned to the $^1B_2(n,\sigma^*) \leftarrow \tilde{X}^1A_1$ transition. This absorption system, however, is observed to have an associated vibrational fine structure which is completely characteristic of a Franck–Condon allowed transition. The vibronic structure expected for the $n \rightarrow \sigma^*$ transition, on the other hand, is expected to be dominated by long progressions in ν_2'. The experimental data thus preclude an assignment of the 7.08-eV system to an intravalence transition. The position of the $^1B_1(\sigma n,\pi^*)$ state appears to be satisfactorily accounted for by both the semiempirical and *ab initio* methods in that the vertical transition energies correlate smoothly throughout Table II at 8.3 and 10.0 eV.

While a number of workers have considered the molecular structure of H_2CO in its lower $^1A_2$ and $^3A_2$ states,[15,24,25] only Buenker and Peyerimhoff[18] have looked at the nuclear configurations of the other states in any detail. The results of their PCMO–CI (parent configuration molecular orbital with configuration interaction) treatment are given in Table III. The equilibrium values of the out-of-plane angle which is defined as the angle between the carbonyl bond and the bisector of the HCH angle show the required behavior, in that the (n,π^*), $(\sigma n,\pi^*)$, and (π,π^*) states, which bear the π^* orbital occupancy, are calculated to have a nonplanar molecular configuration. Perhaps the most interesting feature of the Buenker and Peyerimhoff work is their finding that the potential surfaces of the $^1B_2(n,\sigma^*)$, $^1B_1(\sigma n,\pi^*)$, and $^1A_1(\pi,\pi^*)$ states are dissociative in the carbonyl bond stretching direction. This result could provide an explanation for the fact that transitions to these states have not been positively identified in the vacuum ultraviolet. The whereabouts of the $^1A_1(\pi,\pi^*)$ state must remain one of the more important theoretical and experimental problems in the spectroscopy of formaldehyde. Since the π,π^* electronic configuration is incapable of satisfying the normal SCF conditions, the calculated energy of the $\pi \rightarrow \pi^*$ transition is usually overestimated by several eV. Whitten[21] has made a separate and exhaustive study of the $^1A_1(\pi,\pi^*)$ state using extensive CI treatment and has shown that the energy of the vertical $^1A(\pi,\pi^*) \leftarrow \tilde{X}^1A_1$ transition could be as low as 9.9 eV.

The effect of chemical substituents on the nonplanar equilibrium structures and barrier heights of a number of carbonyl-containing compounds which bear the n,π^* electronic configuration has recently been treated by Condirston and Moule.[26] Data from their CNDO/2 calculations is given in Table IV along with the experimental results which are available for these systems. The extreme sensitivity of the barrier height to the nature of the attached group is clearly illustrated in these calculations, with the CH_3 group (BH = 50 cm^{-1}) and the F group (BH = 1900 cm^{-1}), respectively reducing and enhancing the barrier height with respect to H_2CO (BH = 760 cm^{-1}). It is possible to attribute this variation to an inductive effect from the substituent which acts through the σ-bond framework. In the planar C_{2v} molecule the a_1 and b_2 σ MO's are completely separate from the $b_1\pi^*$ MO. In the nonplanar C_s configuration the a_1 and b_1 representations correlate to the a'' symmetry species with the result that the $2p_x$(C) AO is capable of responding to induction through the σ bonds. In the case of F_2CO a net charge flow occurs from the $2p_x$(C) into the 2s(C) AO which, from the Walsh postulate, would explain the very high barrier to molecular inversion.

B. Extravalence States

By extravalence or Rydberg states we mean those electronic states which arise from electronic configurations in which one of the electrons has a principal quantum number which takes a value at least one greater than it has in the ground electronic state. These higher orbitals behave more like atomic orbitals, and they give rise to a Rydberg series of states which converge at a limit which corresponds to the complete removal of the electron. To a good approximation the energies of the Rydberg states can be represented by a Rydberg-type formula

$$E_n = A - R/(n - \delta)^2$$

where *A* is the series limit, *R* the Rydberg constant, *n* the principal quantum number, and δ the quantum defect. For molecules built of atoms of the first period, δ is small: 0.1 for states obtained from *nd* electrons, 0.3–0.5 for *np* electrons, and 0.9–1.2 for *ns* electrons.

Excitation of a single electron from the oxygen nonbonding MO b_2n(O) into the higher Rydberg *ns*, np_x, np_y, np_z orbitals leads to the following set of excited states and electronic configurations:

$(a_1)^2(b_1)^2(b_2)^1(a_1^*)^1$	$^1B_2,^3B_2(n,3s)$
$(a_1)^2(b_1)^2(b_2)^1(b_2^*)^1$	$^1A_1,^3A_1(n,3p_y)$
$(a_1)^2(b_1)^2(b_2)^1(a_1^*)^1$	$^1B_2,^3B_2(n,3p_z)$
$(a_1)^2(b_1)^2(b_2)^1(b_1^*)^1$	$^1A_2,^3A_2(n,3p_x)$

Five further electronic configurations and energy levels arise from the promotion of a b_2n(O) electron into the *nd* Rydberg orbital. Excitation from the other occupied $a_1\sigma n$(CO) and $b_1\pi$(CO) MO's leads to a replication of the manifold of Rydberg states at higher energies whose series limit corresponds to the higher ionization states of H_2CO.

Whitten and Hackmeyer[19] and Peyerimhoff, Buenker, Kammer, and Hsu[20] through the addition of diffuse orbitals into the atomic orbital basis set have extended the *ab initio* MO treatment to include the Rydberg states. The

TABLE IV. Calculated and Experimental Barriers to Inversion and Out-of-Plane Angles for the (n,π^*) State of Some Carbonyl Compounds[a]

Molecule	Barrier (cm^{-1})		Angle (deg)	
	Exptl	Calcd	Exptl	Calcd
F_2CO	>4000	4600		40
HFCO	2800–4200	1900	30–35	38
H_2CO	356	760	33.6	35
C_4H_6O	1550	180		23
CH_3CHO		50		18
HCCCHO	~0	0	0–4	0

[a] Data taken from Condirston and Moule.[26]

TABLE V. Comparison of the Observed and Calculated Transition Energies for the Extravalence (Rydberg) States of Formaldehyde

	Ref 19	Ref 20	Ref 22	Exptl
$^1B_2(n,3s)$	7.48	7.38	7.14	7.08
$^1A_1(n,3p_y)$	8.30	8.11	8.41	7.97
$^1B_2(n,3p_z)$		8.39	7.98	8.14
$^1A_2(n,3p_x)$		9.07	8.63	
$^1B_2(n,4s)$			9.33	9.27
$^1B_2(n,3d_{z^2})$			9.44	
$^1B_1(n,3d)$			9.45	
$^1B_2(n,3d_{xz})$			9.46	
$^1B_2(n,4p_z)$			9.71	9.63

results of their separate calculations are given in Table V. Perhaps the most interesting result to emerge from these studies is that the singlet state which lies immediately above the $^1A_2(n,\pi^*)$ state is not the $^1B_2(n,\sigma^*)$ intravalence state, but is instead the $^1B_2(n,3s)$ Rydberg.

III. $\tilde{X}^1A_1$ Ground State of Formaldehyde

We now come to a description of the various electronic states of formaldehyde and begin here with a discussion of the ground electronic state. As early as 1934, Dieke and Kistiakowsky[27] obtained a ground-state molecular structure for formaldehyde from an analysis of the rotational fine structure contained in six bands in the near-ultraviolet. These authors were able to evaluate the rotational constants A′, A″, B̄′, and B̄″ from the spectrum, and, by assuming that the ground state is C_{2v} and that the HCH angle is 125°, arrived at the values 1.17 and 1.27 Å for the CH and CO bond lengths. Somewhat later these data were reworked by Herzberg[28] who employed an improved value of the ∠HCH constraint. Structures for H_2CO have also been obtained by Davidson, Stoicheff, and Bernstein[29] from an analysis of the infrared spectrum and by Stevenson, LuValle, and Schomaker[30] from an electron diffraction study.

Johnson, Lovas and Kirchoff[31] have recently subjected the microwave frequency data which are available for H_2CO and $H_2{}^{13}CO$[31a-g] to an exhaustive rotational analysis and have compiled critical tables of the frequency data in the 1-MHz–300-GHz region. Reliable values for the molecular parameters such as the rotational constants and centrifugal distortion constants are to be found in their review article. The most accurate structural determination for formaldehyde comes from the work of Takagi and Oka.[32] From an extensive analysis of the microwave spectra of H_2CO, $H_2{}^{13}CO$, $H_2C^{18}O$, HDCO, and D_2CO, after having made corrections for vibrational as well as electronic interaction, these authors obtained as the equilibrium structure of formaldehyde: ∠HCH = 116° 31′, R(CH) = 1.101 Å, and R(CO) = 1.203 Å.

The infrared spectrum of formaldehyde has been studied by Ebers and Nielsen,[33,34] Blau and Nielsen,[35] and Patty and Nielsen.[36] Formaldehyde has six normal modes of vibration, all of which are active in the spectrum. Three of these, ν_1, ν_2, and ν_3, transform under the operations of the C_{2v} point group as a_1 species and induce electronic transition moments along the axis of least moment of inertia (a-type bands). The fourth vibration ν_4 induces a moment along the axis of intermediate moment of inertia (b-type bands) while the remaining ν_5 and ν_6 vibrations are polarized along the axis of largest moment of inertia (c-type bands). All of the fundamental bands have been resolved in the infrared and display rotational features of an axially symmetric top with two moments of inertia large, compared to the third moment (near-prolate symmetric top). The spectrum has interesting features which may be attributed to Fermi resonance and has provided through the interaction of ν_4 and ν_6 the first known example of accidental coriolis resonance.[35] The c-type and b-type coriolis interactions of ν_3 coupling with ν_6 and ν_4 have recently been observed by Nakagawa, Kashiwagi, Kurihara, and Morino,[38] who compared the rotational envelopes of the bands in the infrared spectrum with those obtained from a computer synthesis. Table VI lists the fundamental frequencies of H_2CO, D_2CO, and HDCO in the $\tilde{X}^1A_1$ state while Figure 5 gives a representation of their normal modes.

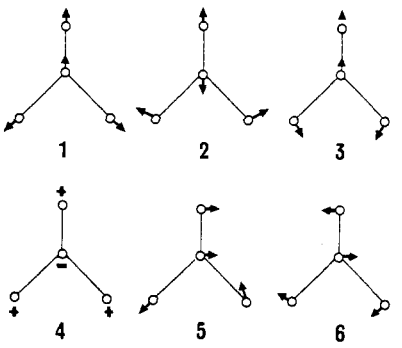

Figure 5. The six normal vibrations of $\tilde{X}^1A_1$ H_2CO. The frequencies (in cm^{-1}) and species of the fundamentals are: $\nu_1(a_1)$ = 2766.4, $\nu_2(a_1)$ = 1746.1, $\nu_3(a_1)$ = 1500.6, $\nu_4(b_1)$ = 1167.3, $\nu_5(b_2)$ = 2843.4, and $\nu_6(b_2)$ = 1251.2.

A number of force constant calculations have been made on formaldehyde.[39,40] An early, yet detailed calculation in which the vibrational frequencies, rotational distortion, and coriolis coupling constants were evaluated from a model force field was made by Oka and Morino.[40a] Somewhat later Shimanouchi and Suzuki[40b] employed the 15 pieces of in-plane frequency data from H_2CO, D_2CO, and HDCO to evaluate by a least-squares procedure, a general harmonic force field for formaldehyde. McKean and Duncan,[40c] however, have pointed out that two reasonable sets of force constants can be obtained for the a_1 block which are equally compatible with the H_2CO and D_2CO frequency data. Their first set of force constants can be identified with the set obtained by Shimanouchi and Suzuki. The Urey–Bradley force field of Miyazawa[41] is of interest in that it demonstrates that while the nonbonded interactions between the two hydrogen atoms are very small, rather large repulsions exist between the hydrogen and oxygen atoms. This force may, in part, explain the fact that the HCH angle in H_2CO is considerably smaller than 120°.

IV. $\tilde{A}^1A_2(n,\pi^*)$ State of Formaldehyde

In absorption H_2CO displays a beautifully sharp absorption spectrum in the near-ultraviolet region, extend-

TABLE VI. Ground-State Fundamental Frequencies of Formaldehyde[a] (cm^{-1})

	H_2CO	D_2CO	HDCO
ν_1	2766.4	2055.8	2844.1
ν_2	1746.1	1700	1723.4
ν_3	1500.6	2105.7	1400.0
ν_4	1167.3	933.8	1059
ν_5	2843.4	2159.7	2120.7
ν_6	1251.2	990.4	1027

[a] Data taken from Job, Sethuraman, and Innes.[42]

ing from 3530 to 2300 Å which was first recorded by Henri and Schou[43] and by Schou.[44] The emission spectrum, which extends over the region 3400 to 4070 Å, was originally observed as a chemiluminescence,[45] and is readily excited either optically[5,6] or in a discharge.[46,47] There is very little outward resemblance between the vibrational structure of the two systems, since it is only a few, very weak bands which are common to the absorption and emission spectra.

The rotational analysis of a number of absorption bands of H_2CO was quickly taken to an advanced state with the brilliant work of Dieke and Kistiakowsky.[27] Their study, made in 1934, may be considered to be the first unambiguous interpretation of the electronic spectrum of a polyatomic molecule. From an analysis of the subband structure for $K \geq 3$ of the six main bands at 3530, 3430, 3390, 3370, 3295, and 3260 Å, these authors were able to show that the moment of the electronic transition was directed perpendicular to the near-symmetric top axis (CO bond direction) and in a direction parallel to a line connecting the hydrogen atoms. They were able to obtain values of the rotational constants A and $\bar{B} = (B + C)/2$ for both the upper and lower excited states, and to establish for the first time a ground-state molecular structure for H_2CO.

The interpretation of the vibrational structure developed more slowly. In absorption, the spectrum is characterized by a series of strong bands which form a number of well-developed progressions in a frequency of 1182 cm^{-1}. This interval was observed to be independent of deuterium for hydrogen isotopic substitution, and it was assigned to ν_2', the normal mode which most closely corresponds to carbon–oxygen valence stretching. Other intervals of 824, 1322, and 2872 cm^{-1} were observed in the early work, and were assigned respectively to ν_4' (the out-of-plane bending mode), ν_3' (the in-plane HCH bending mode), and ν_1' (the symmetrical C–H stretching mode). It has been necessary, however, to subject this interpretation to considerable revision since (a) the major hot bands in the long-wavelength end of the spectrum did not provide satisfactory intervals with which to correlate the frequency data obtained in the infrared work, (b) the band structure within the emission and absorption spectra did not possess the usual mirror image relationship, (c) abnormally small intervals of 125 cm^{-1} appeared in the spectrum, and (d) bands of type a and type c polarizations have been uncovered in the spectra among the more prominent type-b bands.

Since the first excited state in H_2CO may be given the designation $\tilde{A}^1A_2{}^e(n,\pi^*)$, it follows that, under electric dipole selection rules, the transition is forbidden, and that the $v' = 0 \leftarrow v'' = 0$ origin band would be absent in the spectrum. The first cold band of moderate intensity which is given the designation A_0 in the absorption system would have to result from Herzberg–Teller vibronic interaction and would be attached as a single quantum addition to the electronic origin. Dieke and Kistiakowsky[27] showed that this band resulted from a transition moment which was induced in the molecular plane perpendicular to the carbonyl bond direction, and hence the symmetry of the quantum addition can be identified as $b_1{}^v$ since $A_2{}^e \times b_1{}^v = B_2{}^{ev}$. As the vibrational species which belong to the b_1 representation are limited to the single normal mode ν_4, the quantum interval can be uniquely assigned as $\nu_4' + \nu(0\text{–}0)$. In elucidating this point the hot bands at longer wavelengths should be of assistance since it is to be anticipated that the vibrational activity in the cold band progressions in ν_4' should also be reflected in the hot bands involving excitation of ν_4''. The principal hot band, designated by Henri and Schou[43] as α, lies at 1292 cm^{-1} to lower frequencies from the A_0 band. In Table VI ν_4'' is given as 1167 cm^{-1}, and it follows therefore that the excited-state interval in ν_4' is given as 1292–1167 = 125 cm^{-1} which is indeed a very strange result. To test the hypothesis that the A_0 and α bands result from the activity of a single quanta of ν_4' and ν_4'' Dyne[48] made a study of the rotational fine structure of the α band. Since the intensity alteration in the K substructure depends on the statistics of the lower of the two combining vibronic states the transitions $\tilde{A}^1B_2{}^{ev} \leftarrow \tilde{X}^1A_1{}^{ev}$ and $\tilde{A}^1A_2{}^{ev} \leftarrow \tilde{X}^1B_1{}^{ev}$ should have a reversed intensity alteration in their subband structure. With Dyne's observation of the required intensity reversal, the unexpected assignment of ν_4' = 125 cm^{-1} was confirmed. From a study of the temperature dependence of the intensity of the α band, Cohen and Reid[49] concluded that the vibronic transition originated from a vibrational excited level in the $\tilde{X}^1A_1$ state and that it had a Boltzmann factor corresponding to an energy of about 1200 cm^{-1}.

The way out of this difficulty was pointed out by Walsh[9] and was worked out in more detail in an analysis by Brand.[10] If the orbital energies of H_2CO could be correlated against HCH or OCH angle bending in accordance with the postulates of Walsh, the molecular configuration of the $\tilde{A}^1A_2$ state would assume a nonplanar equilibrium structure with the oxygen and hydrogen atoms forming the corners of a pyramid. Such a nonplanar molecule will have two distinct equilibrium configurations which are related to each other by an inversion of the nuclei at the center of mass, irrespective of whether this coincides with a center of symmetry or not. In the case of the unsymmetrical substituted methane derivatives each configuration corresponds to a distinct optical isomer. Here, the configurations correspond to separate minima in the potential function. It is possible to correlate the manifold of energy levels in the double minimum potential function with the height of the barrier separating the minima. This is shown in Figure 6. The evenly spaced energy levels on the right-hand side of this diagram result from the out-of-plane harmonic vibrations of a rigid planar molecule. Since the symmetry of a vibronic wave function (ev) can be obtained as the direct product of the electronic (e) and the vibrational (v) wave functions, the even (+) levels may be labeled $A_1{}^e \times a_1{}^v = A_1{}^{ev}$, while the odd levels are given as $A_1{}^e \times b_1{}^v = B_1{}^{ev}$. The energy levels given on the left-hand side of the diagram are classified under the representations of the C_s point group where A′ is the totally symmetric representation and A″ the representation which is antisymmetric with respect to reflection in the $\sigma(xz)$ plane. As the out-of-plane vibration is totally symmetric in this point group, all of the levels bear the symmetry $A'^e \times a'^v = A'^{ev}$. The evenly spaced energy levels of the planar molecule begin to coalesce as the barrier height is increased until the (+) and (−) levels merge together in the rigid nonplanar case. For

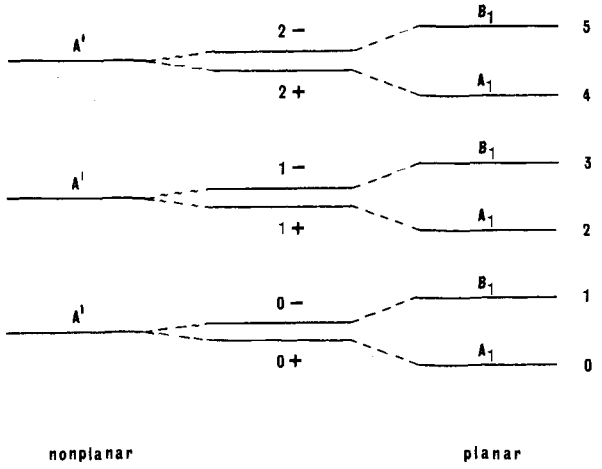

Figure 6. Energy levels of the nonrigid formaldehyde molecule. The symmetry of the electronic wave function is that of the $\tilde{X}^1A_1$ ground state.

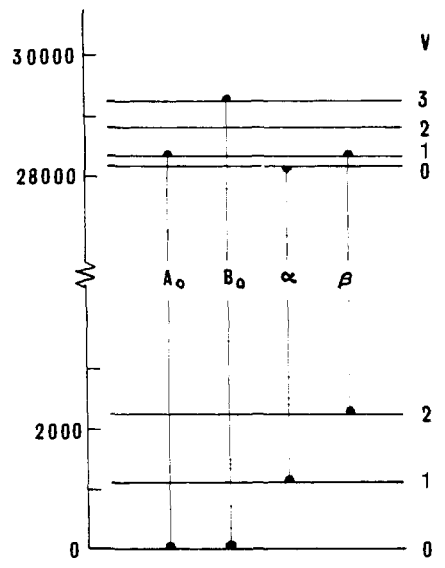

Figure 7. The ν_4' and ν_4'' manifolds of levels in the $\tilde{X}^1A_1$ and $\tilde{A}^1A_2$ electronic states of formaldehyde. The notation of Brand[10] has been used to denote the transitions.

intermediate cases the splitting of the lower components is small but increases rapidly at the top of the potential barrier until it becomes equal to half the separation between the adjacent unperturbed levels. To provide a symmetry label to the levels of the inversion manifold which lie at intermediate barrier heights, it is necessary to consider formaldehyde as a nonrigid system which undergoes large amplitude inversion motion. The symmetry groups of such nonrigid molecules have been discussed by Longuet-Higgins[50] and more recently by Altmann.[51] In the G_4 molecular symmetry group which applies to the nonrigid X_2YZ system under consideration, the four symmetry operations are the identity E, the inversion E*, the permutation (x_1x_2), permutation-inversion $(x_1x_2)^*$. As the G_4 point group is isomorphic to the C_{2v} group, it is possible, therefore, to classify the vibronic levels of the nonrigid H_2CO molecule equally well by the A_1, A_2, B_1, and B_2 irreducible representations of the C_{2v} point group.

Since it is permissible to employ the representations of the C_{2v} group even though the classification is more correctly G_4, the vibronic symmetries of the (+) and (−) levels of the upper state are alternately $A_2^e \times a_1^v = A_2^{ev}$ and $A_2^e \times b_1^v = B_2^{ev}$. Under vibronic selection rules, the transitions $\tilde{A}^1A_2^{ev} \leftarrow \tilde{X}^1B_1^{ev}$ and $\tilde{A}^1B_2^{ev} \leftarrow \tilde{X}^1A_1^{ev}$ are allowed and give rise to moments directed perpendicular to the xz symmetry plane. The y axis corresponds to the b rotational axis and the α, β, A_0, and B_0 bands which bear the above assignment are characterized by a type b rotational envelope. The arrangement of the vibrational levels in the ν_4'' and ν_4' manifolds, their symmetry classifications, and the transitions connecting them are illustrated in Figure 7. From this diagram it is clear that the wave number separation of the A_0 and α bands minus the first quantum of ν_4'' gives the splitting of the first inversion level, that is, $\nu(A_0) - \nu(\alpha) - \nu_4'' = \nu(0-) - \nu(0+) = 125\ cm^{-1}$. The anomalous 125-$cm^{-1}$ interval which had created such intractable problems in the vibronic analysis of the near-ultraviolet bands structure of H_2CO on this basis becomes the inversion splitting of the zero-point level of the $\tilde{A}^1A_2$ state. The 824-cm^{-1} frequency interval which separates the A_0 and B_0 bands in absorption is the difference between the two upper components of the inversion manifold (0−) and (1−).

The fluorescence spectrum of H_2CO is dominated by the activity of the carbonyl stretching mode $\nu_2''(a_1)$ which forms long progressions which run to lower frequencies for several members with positive anharmonicity and then negatively for a few more. The origins of these progressions show no obvious resemblance to the corresponding diagram for the absorption system. Brand[10] has shown how the bands can be grouped into two principal systems which he labels α and β. The α series of bands, of which α is the most prominent member, all originate from the $v' = 0$ level of the $\tilde{A}^1A_2$ upper state and terminate on the odd v levels of ν_4'' of the $\tilde{X}^1A_1$ state; *viz.*, $v' = 0 \rightarrow v'' = 1, 3, \ldots$, while the β series combines a common upper $v = 1$ level with even quanta of ν_4''; *viz.*, $v' = 1 \rightarrow v'' = 2, 4, \ldots$. The A_0 band which bears the assignment $v' = 1 \rightarrow v'' = 0$ occurs very weakly in emission, as a result of its unfavorable Franck-Condon factor. Other band series have been observed in the emission spectrum by Robinson.[52] Interest in the fluorescence spectra of formaldehyde has been rekindled by the recent developments in high-power, pulsed tunable lasers. Yeung and Moore[53] have selectively excited a number of vibronic levels of H_2CO and D_2CO with a high power-pulsed laser. Their tunable ultraviolet light source was based on obtaining a summation frequency by mixing into a nonlinear crystal (potassium dihydrogen phosphate) the 6943-Å output of a ruby laser and the continuously tunable output of an organic dye laser. Their values for the lifetimes of the (1−) and (0−) + $3\nu_2'$ levels of D_2CO of 5 ± 6 μsec and 103 ± 15 nsec, respectively, show a considerable shortening at higher energies, which is ascribed to the effects of predissociation.

To account for the staggering in the stack of energy levels of ν_4', Brand[10] solved the vibrational eigenvalue problem of an anharmonic oscillator in a double minimum potential. The two-parameter model function he selected was of the form

$$V(\theta) = \tfrac{1}{2}K(\Delta\theta)^2$$

which gives rise to two parabolas displaced on either side of the ordinate axis by the equilibrium angle θ_m. In this expression K is the harmonic force constant and $\Delta\theta$ is the change in the out-of-plane angle from either of the equilibrium positions $\pm\theta_m$. When the eigenvalues from this model calculation were fitted to the first three levels of the inversion manifold, the potential function was found to have a value of 720 cm^{-1} for $\theta = 0$ (the barrier height), while the value of θ at the potential minima was $\theta_m = 27°$. As the function climbs to a sharp spike at the top of the barrier, this form of the potential must be re-

TABLE VII. Observed and Calculated $\Delta G(V_4 + {}^1/_2)$ Values of Formaldehyde[a] (in cm^{-1}) for the $\tilde{A}^1A_2$ Excited State

	Least-squares fit of H_2CO data			Predicted Values of D_2CO			Predicted values of HDCO		
v	Obsd	Calcd[b]	Calcd[c]	Obsd	Calcd[b]	Calcd[c]	Obsd	Calcd[b]	Calcd[c]
0	124.6	123.8	123.7	68.5	61.8	61.8	96.5	82.5	82.4
1	417.7	417.3	417.3	318.5	317.1	317.0	368.5	351.3	351.2
2	405.6	406.0	406.1	281.0	270.0	269.6	331.0	318.6	318.4
3		479.2	480.8	348.0	339.4	339.8	347.0	388.9	389.6
4		515.1	518.1	382.0	365.3	366.3	374.0	418.7	420.3

[a] Data taken from Moule and Ramachandra Rao, ref 58. [b] Quadratic plus Gaussian. [c] Quadratic plus Lorentzian.

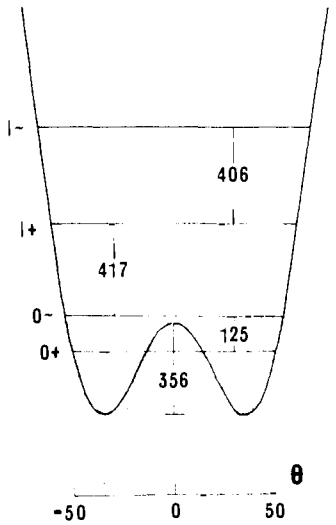

Figure 8. The double minimum potential function of the $\tilde{A}^1A_2$ electronic state of formaldehyde and the vibrational levels of the ν_4' manifold.

garded as physically unreasonable, since the real barrier should be rounded and somewhat lower. The three-parameter model function

$$V(Q) = \lambda Q^2/2 + A \exp(-a^2Q^2)$$

which may be considered to be a Gaussian function superimposed on a quadratic potential was used by Henderson and Muramoto[54] to overcome the ill conditioning of the earlier function at $\theta = 0$. Eigenvalues for this problem have been tabulated by Coon, Naugle, and McKenzie[55] in terms of a reduced frequency, a variable barrier height, and a shape factor. From a fit of the first four levels to the experimental data these authors obtained an improved value of 385 cm^{-1} for the barrier height. Through the relationship $\theta_m^2 = Q_m^2 G_{44}$ which connects the internal coordinate θ with the normal coordinate Q through the G_{44} element of the Wilson's **G** matrix,[56] Henderson and Muramoto evaluated θ_m at 20.7°. While the foregoing two models do take account of the effect of large angle bending on the shape of the potential function, they both use a constant form for the kinetic energy. That is, maintaining G_{44} constant throughout the inversion process is tantamount to employing a set of coordinates for the inverting atoms which are completely rectilinear. Jones and Coon[57] circumvented this difficulty by redefining the relationship in differential form, $dQ = G_{44}(\theta)^{1/2}d\theta$, which allows the reduced mass to vary as a function of θ. While their values for the barrier height of 336 cm^{-1} was not all that different from the preceding calculation, they did find that θ_m increased to 33.6°. The double minimum potential function for the $\tilde{A}^1A_2$ state of formaldehyde showing the energy levels is illustrated in Figure 8.

Extensive calculations have also been carried out by Moule and Ramachandra Rao.[58] These authors derived an expression for the Hamiltonian of a rotating–vibrating–inverting tetratomic system in which one curvilinear coordinate corresponding to the inversion motion of the two hydrogen atoms and five rectilinear coordinates for the remaining degrees of vibrational freedom were employed. Two model potential functions were used in the separate calculations, one consisting of the sum of quadratic and Gaussian functions which was identical with the two preceding-well functions, while in the second calculation, the Gaussian barrier term was replaced by a Lorentzian term

$$V(\theta) = {}^1/_2K\theta^2 + K_B/(c^2 + \theta^2)$$

Here K is the usual quadratic force constant, c and K_B are shape parameters, and θ is the out-of-plane angle. The results of the two sets of calculations are shown in Table VII where the least-squares parameters refined for H_2CO were transferred to the isotopic species HDCO and D_2CO. That the Gaussian and Lorentzian functions provide equally good potentials for the inversion motion of formaldehyde is illustrated by the barrier heights in the two cases which are, respectively, 354.53 and 354.43 cm^{-1}.

A. Type-a Parallel Bands

In their pioneering study Dieke and Kistiakowsky[27] detected the presence of weak bands in the near-ultraviolet system which were polarized in a direction parallel to the near-symmetric top axis (CO bond direction). That these bands were invariably associated with transitions which terminated on the lower positive components of the ν_4 inversion manifold was demonstrated by Brand[10] some time thereafter. In particular, one of these bands was found to correspond to the 0–0 transition, that is, a transition which originated on the $v'' = 0$ level of the $\tilde{X}^1A_1$ state and terminated on the (0+) level of the $\tilde{A}^1A_2$ state. Such a transition may be represented as $\tilde{A}^1A_2{}^{ev} \leftarrow \tilde{X}^1A_1{}^{ev}$ and is rigorously forbidden by electronic as well as vibronic selection rules. Several suggestions were put forward to explain the appearance of such bands in the absorption spectrum. Pople and Sidman[59] explored the possibility that these bands were the outcome of a rotational–electronic interaction about the CO bond axis which mixed the wave functions of the $^1A_2(n,\pi^*)$ state with those of the $^1A_1(\pi,\pi^*)$ state. For this mechanism, Pople and Sidman predicted that the intensity of the K-type subbands for low values of K would be abnormal and that the $K = 0$ subband would be absent from the spectrum altogether. Shortly thereafter Sidman[60] also postulated that the type-a bands might arise as a magnetic dipole transition. In this case the band should appear like any of the other vibronic bands and the intensity distribution of the rotational fine structure should be regular. These alternative proposals were explored by Callomon and Innes[61] who chose to make a rotational analysis of the H_2CO (1+) band at 28,730.34 cm^{-1} which is the least overlapped of the bands of type-a polarization. A portion of this band in

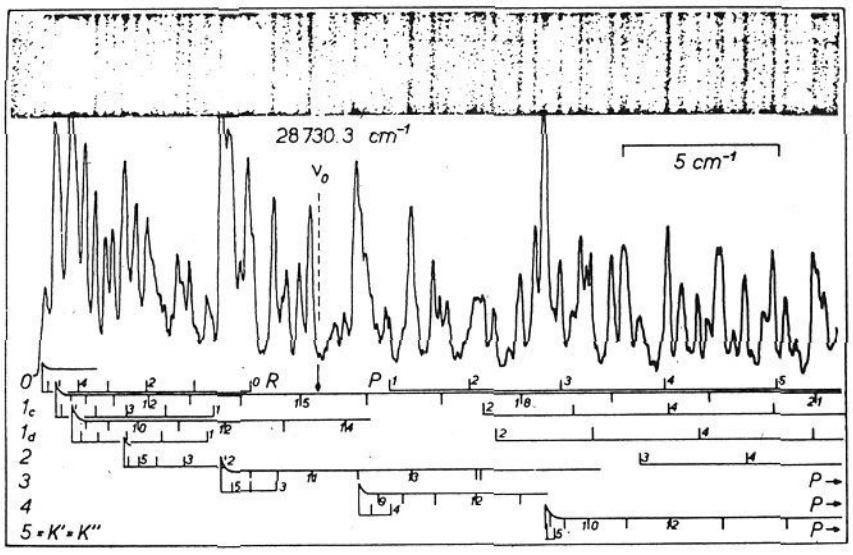

Figure 9. The type-a, 4_0^2 band of H_2CO (Callomon and Innes, ref 61).

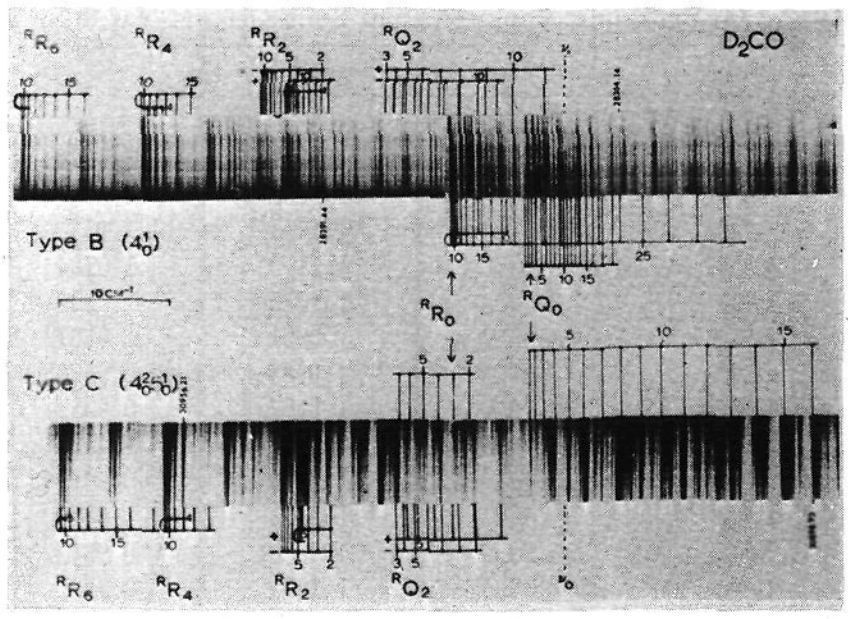

Figure 10. Central portions of two perpendicular bands of D_2CO. The type-b 4_0^1 band centered at 28,369.44 cm^{-1} and the type-c $4_0^2 5_0^1$ band at 30,921.54 cm^{-1} (Job, Sethuraman, and Innes, ref 42).

TABLE VIII. Polarizations of the Bands

Change in vibrational quantum number a_1	b_1	b_2	$\Gamma(\psi'_{ev} + \psi''_{ev})$	Band type
Unrestricted	Even	Even	A_2	a (magnetic) (dipole)
Unrestricted	Even	Odd	B_1	c
Unrestricted	Odd	Even	B_2	b
Unrestricted	Odd	Odd	A_1	a

the region of the vibronic origin is shown in Figure 9. Callomon and Innes found that the frequencies and relative intensities of the rotational fine structure of the (1+) band were fully compatible with what would be expected for the type-a transitions in a near-prolate top in that the subbands $K = 0, 1, 2$ were present with normal intensity. They estimated that the leading type-a bands had about 3–5% the intensity of the leading type-b bands which corresponded to an f value of the parallel subsystem of 3×10^{-6}. This observed oscillator strength is equivalent to a magnetic dipole strength of about 2 BM which is in close agreement to the theoretical value of Mason[62] who evaluated the magnetic dipole moment at the near-ultraviolet system of formaldehyde by an LCAO–MO method to be 1.1 BM. From a variety of separate experimental sources, Callomon and Innes were led to select the second of the Sidman mechanisms to explain the appearance of the parallel system; namely, that the magnetic dipole strength in formaldehyde is sufficiently large that it can manifest itself against the rest of the singlet system, which itself is zeroth order forbidden by the transformation properties of the $b_2n(O)$ and $b_1\pi^*(CO)$ MO's.

B. Type-c Bands

The near-ultraviolet absorption system in formaldehyde, assigned to an $n \rightarrow \pi^*$ electron promotion, is forbidden as a pure electronic transition. An approximate calculation of the borrowing (or stealing) of intensity from the adjacent allowed transitions into the near-ultraviolet system has been given by Pople and Sidman.[59] In their analysis, admixture of the $^1B_2(n,\sigma^*)$ electronic wave function into the $^1A_2(n,\pi^*)$ wave function, through the vibrational interaction of the $\nu_4(b_1)$ mode, was held to be responsible for the oscillator strength of the b-polarized transitions. c-Polarized transitions were taken to result from a perturbation of the $^1B_1(n\sigma,\pi^*)$ and $^1A_2(n,\pi^*)$ electronic wave functions through the interaction of the $\nu_5(b_2)$ and $\nu_6(b_2)$ modes of vibration. Table VIII summarizes the expected polarizations of the bands in the $\tilde{A}\,^1A_2 \leftarrow \tilde{X}\,^1A_1$ transition for even or odd changes of the three vibrational species. Pople and Sidman's calculations showed that the dominant pathway for intensity borrowing was through the interaction of the $\nu_4(b_1)$ mode, and that the oscillator strength of the y-polarized transition is 3×10^{-4}, a value which compares favorably with the observed f number of 2.4×10^{-4}. The contribution from the x-polarized transitions was predicted to be 7.2×10^{-7} which would represent 0.3% of the total intensity.

The distinction between type-b and type-c bands is not all that self-evident for a near-symmetric top like formaldehyde, and it is only for the $K = 0$, 1, 2, and 3 subbands that asymmetric top behavior is apparent. This is especially true for a perpendicular type band where it is only in the subband involving $K = 1$ that the effect of asymmetry can be clearly recognized. When Parkin and Poole[63] attempted a rotational analysis of the band which Brand had labeled $(0-) + \nu_3$, they noticed that the central features were different from those of the other perpendicular bands in the spectrum. In particular, this band was observed to be lacking a head in the $^RR_0$ branch at low values of J. Callomon and Innes[61] took up this problem and were able to assign features in the rotational fine structure of this band to the $^RQ_1$ branch. Such an assignment is compatible only for type-c selection rules. Figure 10, which displays central portions of two perpendicular bands of D_2CO, illustrates this point. Callomon and Innes were led to reassign this band to $(0+) + \nu_6'$. From their plates, they estimated that the type-c subsystem could contribute as much as 25% of the observed oscillator strength of the near-ultraviolet system, which is well outside Sidman's prediction of 0.3%. It should be noted here that Sidman assumed that the strength of the b-polarized system was the result of a vibrational perturbation of the $^1A_2(n,\pi^*)$ state at 4.3 eV by the $^1B_2(n,\sigma^*)$ state at 7.1 eV. The discussion given in Sections II.A and VII of this review, however, shows that the location of the $^1B_2(n,\sigma^*)$ state has not been fixed with any certainty, and that in all probability it lies at quite high energies. As a perturber for the $^1A_2(n,\pi^*)$ state, we suggest that the $^1B_2(n,3s)$ at 7.08 eV and perhaps the higher $^1B_2(n,np_z)$ Ryberg states could be likely candidates. An exhaustive analysis of the rotational fine structure of 34 vibronic bands of H_2CO, HDCO, and D_2CO has been carried out by Job, Sethuraman, and Innes.[42] The results of their work are given in Table IX which contains vibrational assignments, rotational constants, and band origins. The notation for the vibronic assignments is due to Brand, Callomon, and Watson.[64] Excited-state fundamentals are given the same numbers as in the ground state. A given vibrational tran-

TABLE IX. Rotational Constants and Band Origins[a] for the $A^1A_2 \leftarrow \tilde{X}^1A_1$ Electronic Transitions in H_2CO, D_2CO, and HDCO

Band	A'	B'	C'	$D_K' \times 10^4$	$D_{JK}' \times 10^5$	$D_J' \times 10^6$	Origin
				H_2CO			
4_1^0	8.9519	1.1239	1.0044	6.51	6.77	2.79	27020.96
4_0^1	8.7518	1.1242	1.0122	5.05	6.18	3.23	28312.58
4_0^2	8.618	1.1217	1.0117				28730.34
4_0^3	8.5370	1.1179	1.0184	−34.6	12.8	2.71	29135.89
$4_0^2 6_0^1$	8.9022	1.1225	1.0130	5.45	6.92	2.60	29634.25
$2_0^1 4_0^3$	8.1979	1.1051	1.0107	−26.3	9.96	6.18	30340.15
$2_0^2 4_0^1$	8.6426	1.0983	0.9938	3.11	4.69	3.51	30658.58
$2_0^1 4_0^2 6_0^1$	8.7957	1.1157	0.9969	7.79	6.24	2.47	30818.80
5_0^1	8.6932	1.1246	1.0123	18.97	2.11	3.78	31156.28
$1_0^1 4_0^1$	8.7647	1.2340	0.9019	4.77	3.68	19.93	31158.99
$2_0^2 4_0^3$	7.9553	1.1013	1.0049	−17.3	10.4	5.15	31531.61
$2_0^3 4_0^1$	8.5930	1.0860	0.9842	2.48	7.30	2.32	31808.63
$1_0^1 4_0^3$	8.6396	1.1052	0.9781	−0.97	−2.68	−4.04	31987.25
$2_0^1 5_0^1$	8.7419	1.1150	1.0001	13.6	6.96	3.74	32334.64
$3_0^1 4_1^2$	8.1494	1.1055	1.0355	−1.14	7.35	1.52	28450.10
4_1^0	9.3440	1.2758	1.1427	7.05	5.77	3.62	27020.96
	9.40529	1.29537	1.13423	6.354	4.359	2.326	
				D_2CO			
4_0^1	4.4690	0.9563	0.8024	1.26	3.40	1.49	28369.44
4_0^3	4.2634	0.9505	0.8073	−4.07	1.94	2.10	28969.52
$2_0^1 4_0^3$	4.1933	0.9385	0.8008	−11.2	−9.28	1.63	30147.62
$2_0^2 4_0^1$	4.4862	0.9375	0.7883	1.68	3.07	1.62	30700.57
$4_0^2 5_0^1$	4.3970	0.9497	0.7990	1.58	1.40	2.11	30921.54
$1_0^1 2_0^1 4_0^1$	4.4554	0.9451	0.7929	1.87	5.94	1.02	31608.98
$1_0^1 2_0^1 4_0^3$	3.9626	0.9171	0.8044	−64.2	−67.9	0.50	32219.31
	4.72566	1.07698	0.87359	1.655	1.943	1.273	
				HDCO			
4_1^0	6.2157	1.0247	0.8866	3.96	4.00	0.59	27184.79
4_0^1	6.1482	1.0265	0.8942	3.21	4.07	2.43	29339.69
4_0^3	6.1591	1.0248	0.8965	−5.26	7.11	2.99	29039.24
$3_0^1 4_0^1$	6.2407	1.0279	0.8952	0.90	−2.27	8.37	29116.95
$2_0^1 4_0^1$	6.2188	1.0136	0.8948	4.84	0.21	0.64	29529.08
1_0^1	6.1806	1.0283	0.8892	3.28	5.74	1.86	31167.40
4_1^0	6.4393	1.1593	0.9907	5.54	4.40	3.09	27184.79
6_1^0	6.7326	1.1329	1.0080	−1.35	4.92	−8.13	27215.05
	6.60863	1.16447	0.98608	3.660	2.801	1.773	

[a] Data taken from Job, Sethuraman, and Innes.[42]

TABLE X. Fundamental Frequencies of Formaldehyde[a] (cm^{-1}) for the $\tilde{A}^1A_2$ Excited State

	H_2CO	D_2CO	HDCO
ν_1	2847	2079	2924
ν_2	1173	1176	1189
ν_3	887	(625)	778
ν_4	124.6	68.5	96.5
ν_5	2968	2233	2154
ν_6	904	705	737

[a] Data taken from Job, Sethuraman, and Innes.[42]

sition can then be labeled in the form $m_b^a n_d^c \ldots$ where m, n, ... designate the modes by their numbers, while the superscripts a, c, ... and subscripts b, d, ... give the vibrational quantum numbers in the upper and lower states. The origin band is still called the 0–0 band. The values Job, Sethuraman, and Innes obtained for the fundamental frequencies of formaldehyde in the $\tilde{A}^1A_2$ state are collected in Table X. The current status of the vibrational analysis can be recapitulated as follows.

ν_1', ν_5'. In Brand's original assignment[10] of ν_1' in the spectra of H_2CO and D_2CO, he identified combination bands of the type $1_0^1 4_0^1$, $1_0^1 4_0^3$, etc. Callomon and Innes,[61] however, pointed out that the H_2CO band assigned as $1_0^1 4_0^1$ is of type-c polarization, and consequently changed the assignment to 5_0^1. The detailed analysis of this region by Job, Sethuraman, and Innes[42] revealed that there are actually two bands present here of differing polarization which are separated by only 2.7 cm^{-1}. The high-frequency band they showed to be of type-b polarization, and assigned to the activity of $(0-) + \nu_1'$, $1_0^1 4_0^1$ while the band at lower frequency, of type-c polarization, was assigned to $(0+) + \nu_5'$, 5_0^1.

ν_2'. Much of the near-ultraviolet absorption spectrum is accounted for by the building up of successive quanta of ν_2' The progressions in ν_2' were identified very early on in the analysis of this system through their invariance with respect to isotopic substitution: 1173, 1176, and 1189 cm^{-1}, respectively, for the species H_2CO, D_2CO, and HDCO.

ν_3, ν_6. Some of the bands originally assigned as combinations involving ν_3' were shown by Callomon and Innes[61] to have band types which were only compatible with type-c polarizations. In fact, none of the cold bands observed in the spectra of H_2CO or D_2CO can be assigned directly to quanta of ν_3'. A type-b band is observed in the spectrum of HDCO which is given the assignment $3_0^1 4_0^1$, while in the spectrum of H_2CO a hot band of the correct polarization is attributed to $3_0^1 4_1^2$, from which the ν_3' values of Table X are extracted.

ν_4'. The assignment by Brand[10] of the first four cold bands in the spectra of H_2CO and D_2CO as transitions to 0+, 0−, 1+, and 1− is unambiguous, and, in the pres-

TABLE XI. Geometrical Structures[a] for the Excited States $\tilde{A}^1A_2$ and $\tilde{a}^3A_2$ and the Ground State $\tilde{X}^1A_1$ of Formaldehyde

	$\tilde{A}^1A_2$		$\tilde{a}^3A_2$		$\tilde{X}^1A_1$	
	H_2CO	D_2CO	H_2CO	D_2CO	H_2CO	D_2CO
θ, deg	33.6	33.1	37.9	37.9	0.0	0.0
HCH, Å	118.0	117.9	118.0	118.0	116.52	116.62
C-H, Å	1.0947	1.0947	1.0962	1.0962	1.1161	1.1117
C-O, Å	1.3252	1.3252	1.3069	1.3069	1.2078	1.2078

[a] Data taken from Jones and Coon.[57]

ent notation, corresponds to $0\text{-}0,4_0^1$, 4_0^2, and 4_0^3. In the spectrum of D_2CO, Job, Sethuraman, and Innes[42] have observed two further members of this progression.

Sethuraman, Job, and Innes[65] returned to the formaldehyde problem to examine the perturbations which were apparent under high resolution. In particular, they were interested in the spectrum of H_2CO at (0+) + 2950 cm^{-1} which had been assigned as $1_0^1 4_0^{1\ 10}$ and as 5_0^1.[61] Sethuraman, Job, and Innes showed, in fact, that both of these assignments were correct and that both type-b and type-c polarizations were present. Their analysis revealed that the anomalies in the intensities and frequencies of the fine structure could be attributed to an a axis coriolis coupling between $\nu_4 + \nu_1$ and ν_5 with $A_{eff}\zeta = 0.06$ cm^{-1}.

C. Structure of the $\tilde{A}^1A_2$ Excited State

Since the structure of the $\tilde{A}^1A_2$ state is fixed by four independent parameters, namely, the CO and CH bond distances, the HCH and out-of-plane angle θ, the geometrical configuration cannot be uniquely determined from the *A*, *B*, and *C* rotational constants resulting from the analysis of a single vibronic band. The structures which have been obtained have either assumed a value for one of these parameters, such as the CH bond length,[10,66,67] or have been derived from additional isotopic data.[42] The large amplitude bending motion of ν_4, however, precludes such rigid molecule treatments since not only is θ different for the 0+, 0−, 1+, . . . levels of the inversion manifold, but for each isotope as well. Jones and Coon[57] set out to determine a single structure for formaldehyde which would account for the variation in the rotational constants among the levels of the $\tilde{A}^1A_2$ state. These authors were able to evaluate the *A*, *B*, and *C* rotational constants for the 0+, 0−, 1+, and 1− levels as the expectation values of the reciprocal moments of inertia I_A, I_B, and I_C from the vibrational wave functions which resulted from a fit of a Gaussian + quadratic model function to the potential function which described ν_4. As this technique fixed the value of θ for each inversion level, they were then able to calculate the three remaining structural parameters from the rotational constant data. The best molecular structure for $\tilde{A}^1A_2(n,\pi^*)$ formaldehyde obtained in this way is given in Table XI along with structures for the $\tilde{X}^1A_1$ and $\tilde{a}^3A_2(n,\pi)$ states, for the purposes of comparison.

The gross change in equilibrium structure which formaldehyde undergoes when it is excited from the $\tilde{X}$ ground state to the $\tilde{A}$ excited state appears to be well accounted for in the recent *ab initio* calculations of Buenker and Peyerimhoff[18] who placed the out-of-plane angle in the upper state at 32.7° and the change in carbonyl bond length at +0.29 Å. The corresponding experimental values are 33.6° and +0.12 Å. The nonplanar configuration of $\tilde{A}$ formaldehyde can be interpreted with the aid of the Walsh diagram as has been discussed earlier. In this qualitative picture it is the presence of the electron in the π^* orbital which is held to be responsible for stabilizing the nonplanar configuration. The structural changes which occur in the CO bond can likewise be attributed to the partially filled π^* orbital. The extension of the CO bond length and the drop in ν_2 carbonyl stretching frequency from 1746 to 1173 cm^{-1} on excitation is commensurate with a change in bond order of the CO group of 2 to 1.5 which can be attributed to a cancellation of a π bonding electron by the π^* antibonding electron. This way of looking at the structural changes which occur in an $n \rightarrow \pi^*$ transition as a two stage process in which (a) an electron is lifted from the n orbital and (b) then fed into the π^* orbital is of some value, since it is possible to examine the structural changes which occur in each step individually. Precise information about step (a) can be obtained from the photoelectron data on H_2CO. The first bonded system which appears in the photoelectron spectrum at 10.88 eV has been assigned to the ionization of an $n(b_2)$ electron, $^2B_2(n) \leftarrow \tilde{X}^1A_1$, or to the loss of the nonbonding electron centered on the oxygen atom. While this system does display all of the characteristics of a Franck-Condon allowed transition, the frequencies of the ion are somewhat different from those of the neutral molecule; *viz.*, ν_1'/ν_1'' (2560)/(2766), ν_2'/ν_2'' (1590)/(1746), ν_3'/ν_3'' (1210)/(1500). That the ν_1(CH) stretching mode is lower in the $^2B_2(n)$ ionic state than it is in the $\tilde{X}$ ground state is an indication that the $n(b_2)$ nonbonding orbital is more than a simple AO centered on the oxygen atom and that it does extend into, and provide for bonding, in the CH bonds. The increase in ν_1 stretching frequency on excitation from the $\tilde{X}$ to the $\tilde{A}$ states, ν_1'/ν_1'' (2874)/(2766), along with the decrease in CH bond length, r'/r'' (1.095)/(1.116), is somewhat unexpected since on the basis of process (a) the frequency and bond-length changes would be expected to occur in the reverse directions. The reduction of the CH bond length in the $\tilde{A}^1A_2$ state must be attributed to the presence of the π^* electron (process (b)) which, through an interaction of the σ(CH) and π^* MO's, has the effect of stabilizing the CH bonds. In the distorted C_s configuration the σ and π^* MO's correlate with each other. The HCH angle, on the basis of (a), should be somewhat different in the $\tilde{A}$ state from what it is in the $\tilde{X}$ state since the vibronic band assigned to ν_3' in the photoelectron spectrum has appreciable activity. The loss of the n electron here should effectively reduce the magnitude of the nonbonded repulsions between the oxygen and hydrogen atoms and thereby allow the HCH angle to open to a larger value in the ionic state. In the near-ultraviolet spectrum, ν_3' was not observed as a single quantum addition, and in the structural calculations of Jones and Coon[57] the HCH angle was calculated to be essentially the same as the ground state. Process (b), the addition of the π^* electron, therefore, must offset the structural change resulting from the loss of the n electron. This would appear to be reasonable since the Walsh diagram predicts that the π^* orbital should close the HCH angle.

D. Electric Field Studies

The dipole moment of H_2CO in its various electronic states can, in principle, be obtained from the Stark split-

TABLE XII. Pathways for the Spin-Orbit Coupling of the $\tilde{a}^3A_2(n,\pi^*)$ State to the Higher Intravalence States of Formaldehyde

Component of H_{so}	Species of H_{so}	Perturbing state	Induced moment	Polarization
$H(x)$	B_2	$B_1(\sigma n,\pi^*)$	B_1	x
$H(y)$	B_1	$B_2(n,\sigma^*)$	B_2	y
$H(z)$	A_2	$^1A_1(\pi,\pi^*)$	A_1	z

tings of the lines in the optical spectrum. Such information was obtained initially for the $\tilde{A}^1A_2$ state by Freeman and Klemperer[94,95] who studied the effect of a static field on the rotational fine structure of the H_2CO band at 3390 Å. While they were unable to observe the individual Stark components on their high-resolution plates, they found that the frequency and intensity distribution of the m components within each line did produce an unresolved doublet, from which they were able to derive a dipole moment of 1.56 ± 0.07 D. This is to be compared with the $\tilde{X}^1A_1$ microwave value of 2.33 ± 0.02 D.[96] The change in dipole moment is in the anticipated direction, but somewhat smaller in magnitude than what would be expected from a naive consideration that the electron is transferred from a p orbital on the oxygen atom to an antibonding π^* orbital centered midway in the carbonyl bond. Stark effects may also be used as an aid in the rovibronic assignment since the direction of the transition moment can be uniquely defined from the Stark patterns which result from polarizing the incident radiation in two orthogonal directions. Lombardi, Freeman, and Klemperer[97] used this aspect of the Stark effect to show that the m components of the band assigned to 4_0^2 displayed all of the characteristics expected of a magnetic dipole transition. They observed that the lines of the P and R branches were split into two components when observed with parallel polarized light radiation while with perpendicular polarized light the Q branch lines separated into two components. This observation is a direct confirmation of the earlier assignment of Callomon and Innes[61] of the subsystem of parallel bands to a magnetic dipole transition. Stark effects in formaldehyde have also been observed with alternating electric fields by Bridge, Haner, and Dows[98,99] and Buckingham and Ramsay.[100] The resulting spectrum which is known as an electric field spectrum provides a useful aid in the assignment of the rotational quantum numbers since the Stark perturbation is greatest for the lower J quantum numbers in a given K subband, and hence the first members with each subband appear strongly in the spectrum.

E. Magnetic Field Studies

The effect of a magnetic field on the ultraviolet spectrum of H_2CO was first observed by Kusch and Loomis.[101] In their experiment an absorption cell containing H_2CO vapor was placed into the central portion of a solenoid between a pair of linear polarizers set in a crossed configuration. When an axial field was applied to the sample, those transitions which are magnetically sensitive rotate the plane of the incident polarized light and pass through the analyzing polarizer into the spectrograph. In the H_2CO system, Kusch and Loomis observed an MRS effect only in a narrow region about 3260 Å. Since the fine structure which was evident here did not fit into any regular pattern and the magnetic activity was found for only a single band in the spectrum, these workers assigned the MRS to a perturbation of the upper singlet state by an underlying magnetically sensitive state. At longer path lengths and higher H_2CO pressures, Eberhardt and Renner[102] observed a more extensive MRS system in the longer wavelength 3700–3960 region. The bands here displayed a one to one correlation with the bands Robinson[52] had observed earlier in absorption and were assigned to the $\tilde{a}^3A_2 \leftarrow \tilde{X}^1A_1$ transition, identifying the perturber at 3260 Å as the $\tilde{a}^3A_2$ state. In their high-resolution studies on H_2CO, Parkin, Poole, and Raynes[103] established that local perturbations occurred in the K = 0, 7, 8 submanifolds of the 3260-Å band. The perturbation for K = 0 was initially attributed to a vibrational perturbation, but this was shown to be unsatisfactory by Job, Sethuraman, and Innes[42] who evolved an alternative analysis in terms of a high-order vibration–rotation interaction between the 2^24^1 and 4^26^1 levels. Brand and Stevens[104] have recently made a thorough Zeeman study of the rotational lines in this magnetically sensitive band and have shown that the perturber is indeed the $\tilde{a}^3A_2$ state and that it is the separate 1^12^2 and $1^12^24^1$ levels of the $\tilde{a}$ state which are interacting with the vibronic 2^24^1 level of the $\tilde{A}^1A_2$ state. The interaction involving $1^12^24^1$ was assigned to a spin–rotation intersystem coupling mechanism while the perturbation of the 1^12^2 level was attributed to vibronic spin–orbit coupling. That intersystem crossing can occur between the $\tilde{a}^3A_2$ and $\tilde{A}^1A_2$ states in the absence of an external perturbation has significant photochemical consequences and it is to be expected that the lifetimes of the rotational states in the vicinity of a singlet–triplet perturbation should show irregular variations in their lifetimes.

V. $\tilde{a}^3A_2(n,\pi^*)$ State of Formaldehyde

Among the very weak bands on the low-frequency side of the near-ultraviolet system are a few bands which persist at very low temperatures and do not fit into the vibrational scheme of the $\tilde{A}^1A_2 \leftarrow \tilde{X}^1A_1$ system. These were first observed by Cohen and Reid[49] and soon afterwards by Brand[10] and Robinson.[52] The bands were found to have a rotational envelope which was different from those of the singlet system at shorter wavelengths, and it was recognized immediately that the excited state must be different from that of the main system and that it was most likely $\tilde{a}^3A_2$.

According to the spin selection rule, $\Delta S = 0$, the $\tilde{a}^3A_2 \leftarrow \tilde{X}^1A_1$ transition is forbidden. This is true for electric dipole radiation so long as the electronic wave function can be separated into a spin and a space-dependent part. A coupling of the magnetic field due to the orbital motion of the electron and the spin magnetic moment of the electron, however, is capable of breaking down the space-spin factorization. If a triplet state $\tilde{T}$ is perturbed by a singlet state $\tilde{S}$, then according to McClure,[68] the matrix element for the transition $\tilde{T} \leftarrow \tilde{X}$, where $\tilde{X}$ is the ground state, is given by

$$\langle\psi(\tilde{T})|H_{so}|\psi(\tilde{S})\rangle\langle\psi(\tilde{S})|P|\psi(\tilde{X})\rangle/(E(\tilde{S}) - E(\tilde{T}))$$

Such a perturbation will not occur unless the spin–orbit operator, H_{so}, gives the first integrand the transformation properties of the totally symmetric A_1 species. Since the components of the orbital part of H_{so} transform under the operations of the C_{2v} group as rotations about the x, y, or z axes, the components may be classified respectively as B_2, B_1, or A_2. $\psi(\tilde{T})$ transforms as A_2, and hence the perturbing singlet $\tilde{S}$ in the first integrand may be either $^1B_1$, $^1B_2$, or $^1A_1$ according to the R_x, R_y, or R_z transformation properties of H_{so}. Table XII illustrates this point. An approach which has commonly been used is to employ experimental data for the transition moments,

$\langle\psi(\tilde{S})|P|\psi(\tilde{X})\rangle$ and the perturbation gap, $E(\tilde{S}) - E(\tilde{T})$, and to calculate the matrix elements $\langle\psi(\tilde{T})|H_{so}|\psi(\tilde{S})\rangle$ from a set of wave functions which are derived from semiempirical MO's.

The source of the $\tilde{a}^3A_2 \leftarrow \tilde{X}^1A_1$ transition strength has been considered by a number of workers from this point of view. In the first of such calculations, Sidman[69] transferred experimental data from the vacuum ultraviolet spectrum of acetone to estimate the magnitude of the perturbation gap and the *f* values for formaldehyde. His calculations showed that a mixing of the $\tilde{a}^3A_2(n,\pi^*)$ and $^1A_1(\pi,\pi^*)$ states, through the R_z component of H_{so}, should induce an oscillator strength of 1.5×10^{-7} into the spin-forbidden system. This would be the dominant pathway for singlet–triplet intensification, since the routes which involve a coupling of the R_x and R_y components to the higher $^1B_1(\sigma n,\pi^*)$ and $^1B_2(n,\sigma^*)$ electronic states were found to be at least 100-fold less effective. The vibronic structure of the $\tilde{a}^3A_2 \leftarrow \tilde{X}^1A_1$ transition, he concluded, should have the same characteristics as those of the allowed $^1A_1 \leftarrow \tilde{X}^1A_1$ transition. Somewhat more extensive treatments of this problem have been given by Hameka and Oosterhoff,[70] El-Sayed,[71] Caroll, Van Quickenborne, and McGlynn,[72] Yonezawa, Kato, and Kato,[73] and Ellis, Squire, and Jaffé,[12] which are all in qualitative agreement with the early work of Sidman in that they find the major pathway for single–triplet intensification to involve an R_z coupling of the $\tilde{a}^3A_2$ and $^1A_1(\pi,\pi^*)$ states. The most comprehensive of these calculations are those of Ellis, *et al.*,[12] who used a semiempirical MO method (CNDO/S) to evaluate all of the factors which go to make up the transition moment integrals and the perturbation gap. Their findings are that while the bulk of the singlet–triplet strength should be polarized in a direction parallel to the carbonyl bond, a component which lies in a perpendicular direction should be spectroscopically observable. Indeed, their calculations show that as much as 40% of the induced transition strength could be polarized in the out-of-plane direction. An experimental estimate of the *f* value of the $\tilde{a}^3A_2 \leftarrow X^1A_1$ transition has been made by DiGiorgio and Robinson,[74] who compared the relative intensities of the singlet–triplet system with those of the corresponding singlet–singlet system which lies at higher frequencies. From the measured oscillator strength of 2.4×10^{-4} [75] and the estimated intensity ratio of 1/200 for the two systems, these authors obtained an *f* value of 1.2×10^{-6} for the $\tilde{a}^3A_2 \leftarrow \tilde{X}^1A_1$ system which compares favorably with Sidman's[69] calculated value of $f = 1.5 \times 10^{-7}$.

A. Vibronic Analyses

The foregoing theoretical considerations suggest that most of the strength of the $\tilde{a}^3A_2 \leftarrow \tilde{X}^1A_1$ transition is the result of a spin–orbit mixing of the wave functions of the $\tilde{a}^3A_2$ and $^1A_1(\pi,\pi^*)$ states and that the selection rules should resemble those of a symmetry-allowed, *z*-polarized, transition. Vibronic transitions from the ground-state zero-point energy level, $v'' = 0$, therefore will connect to the $v' = 0, 2, 4, \ldots$ levels of the ν_4 inversion manifold to give rise to bands which are polarized along the axis of least moment of inertia. This behavior is to be contrasted with the singlet–singlet transition where the odd vibrational quanta of ν_4 in one electronic state combine with even quanta of ν_4 in the other electronic state. The patterns produced by the inversion doublets in the singlet–triplet system are therefore reversed over what they are in the singlet–singlet system.

From the study by Hodges, Henderson, and Coon[76] of some temperature-sensitive bands and from the work of Robinson and DiGiorgio[66] much of the inversion structure of the triplet state has been elucidated. At pressure paths up to 120 m atm and temperatures of 130°, Hodges, *et al.*,[76] were able to identify a number of bands at wavelengths longer than 3960 Å in the spectrum of H_2CO which they assigned to the vibronic transitions 2_1^0, $2_1^0 4_0^2$, 4_1^1, and 4_1^3. The experimental values for the (0−)–(0+) and (1−)–(1+) inversion splittings of 36 and 244 cm^{-1}, respectively, which they obtained for the $\tilde{a}^3A_2$ state are to be compared with the corresponding values of 124 and 407 cm^{-1} for the $\tilde{A}^1A_2$ state. Model calculations have been applied to the inversion data by Jones and Coon[57] who approximated the double-well potential as the sum of Gaussian and quadratic terms. The results of their calculations for H_2CO and D_2CO are given in Table XIII. Their model function yielded a value of 776 cm^{-1} for the barrier height which is nearly twice as high as it is in the corresponding singlet state. The ν_2'(CO) frequency of 1251 cm^{-1} which has been observed for the triplet state is 78 cm^{-1} larger than it is in the singlet state. As this difference is expected to persist throughout the carbonyl series of compounds, DiGiorgio and Robinson[74] suggest that it could be used to provide a check as to the multiplicity of the upper state.

TABLE XIII. Observed and Calculated Inversion Levels[a] of $\tilde{a}^3A_2$ Formaldehyde (Quadratic + Gaussian Potential Function)

	H_2CO		D_2CO	
v	Obsd	Calcd	Obsd	Calcd
0	0.0	0.0	0.0	0.0
1	38.1	38.1		12.3
2	538.2	538.2	448	450.3
3	782	775.2		574.1
4	1172	1174.7	889	887.4
5		1553.9		1155.7

[a] Data taken from Jones and Coon.[57]

B. Rotational Analysis

Under conditions of moderately high resolution, $\lambda/\Delta\lambda = 200{,}000$, Robinson and DiGiorgio[66] observed that the structure of the singlet–triplet bands was exceedingly complex and that each band was characterized by a set of red-degraded heads which were separated by 40 cm^{-1} for both H_2CO and D_2CO. These features they assigned to the separate S form, $\Delta N = +2$, and Q form, $\Delta N = 0$, of a near-prolate symmetric top in a triplet electronic state. To account for the addition of spin angular momentum to the rotational angular momenta of a near-prolate symmetric top, it is necessary to employ the three quantum numbers, *J*, *N*, and *K*. *J* is the quantum number of total angular momentum and takes on the values $N - S, N, N + S$ where the spin quantum number $S = 1$. The rotational transitions are given by $\Delta J = 0, \pm 1$, $\Delta N = 0, \pm 1, \pm 2$, and $\Delta K = 0, \pm 1, \pm 2$. Branches within the *K* subbands are designated as: S form ($\Delta N = +2$), R form ($\Delta N = +1$), Q form ($\Delta N = 0$), P form ($\Delta N = -1$), and O form ($\Delta N = -2$). A line-by-line analysis of several bands of the $\tilde{a}^3A_2 \leftarrow \tilde{A}^1A_1$ transition has been given by Raynes.[67] Raynes obtained values for the rotational constants, rotational distortion constants, spin–spin, and spin–molecular rotation constants for the $^3A_2(O+)$ and $^3A_2(1+)$ levels of H_2CO by a least-squares fitting procedure on the absorption frequency data of Robinson and DiGiorgio. Birss, Dong, and Ramsay[77] recently have rephotographed the singlet–triplet bands under improved conditions of resolving power (500,000) and pressure *X*

path-length (7 atm m) and have considerably extended the assignment and have further refined the spin and rotational constants of the $^3A_2(0+)$ and $^3A_2(1+)$ levels. Under the conditions of highest absorption, they observed very weak lines on the high-frequency side of the S-form branch which could only be assigned to branches of the $\Delta K = \pm 2$ subband. In the Hougen theory[78] the intensities of the $\Delta K = \pm 2$ band relative to those of the $\Delta K = 0$ band depend on the ratio of the transition moments $(\mu B_1 + \mu B_2)/\mu A_1$. From an estimate of the experimental intensities of these two types of subbands Birss, Dong, and Ramsay[77] deduced that the transition moment in a direction perpendicular to the top axis is about 10% of that directed along the axis. This result is in accord with the recent theoretical work of Ellis, Squire, and Jaffé[12] who predicted that the spin–orbit perturbation between the $\tilde{a}^3A_2(n,\pi^*)$ and $B_1(\sigma n,\pi^*)$ states could account for as much as 24% of the oscillator strength of the T–S transition which allows the observed perpendicular component of the transition moment to be identified with the out-of-plane direction.

The higher barrier and lower out-of-plane angle of H_2CO in the $\tilde{a}^3A_2$ state relative to the $\tilde{A}^1A_2$ state, *viz.* (354)/(776) and (33.6)/(37.9), has not been adequately accounted for in recent theoretical work. An appealing rationalization for these dynamical and structural differences results from considering the correlation between the n and π^* electron as the molecule is distorted from the plane. In MO theory, the Fermi correlation energy $2K_{n\pi^*}$, which measures the energy separation between the singlet and triplet states of an equivalent electronic configuration, is expected to increase strongly with nonplanar distortion. The result is that, while the $\tilde{A}^1A_2$ state should be stabilized with increasing distortion, the $\tilde{a}^3A_2$ state should be destabilized. The higher barrier and greater out-of-plane angle in $\tilde{a}^3A_2$ H_2CO is then a result of the vibrational potential governing ν_4' being depressed to lower energy as the hydrogen atoms are displaced from the plane.

VI. Rydberg States of Formaldehyde

The vacuum ultraviolet spectrum of formaldehyde was first studied by Price[79] in 1935 and then later in somewhat more detail by Fleming, Anderson, Harrison, and Pickett,[80] Allison and Walsh,[81] and Bell.[82] Recent interest in the vacuum ultraviolet transitions have stemmed from the discovery of formaldehyde in the interstellar medium by Snyder, Buhl, Zuckerman, and Palmer.[83] The astrophysical implications of this observation have led Gentieu and Mentall[84] and Mentall, Gentieu, Krauss, and Neumann[85] to reinvestigate the 2000–1000-Å region and to make new observations down to 600 Å. This work has been supplemented by the recent inelastic electron scattering spectra of Weiss, Kuyatt, and Mielczarek.[86]

In his pioneering work, Price[79] found that the frequencies of a number of the bands could be fitted into two separate series which converged on to a common series limit. The first series, which took the 1556-Å band as its origin, was followed out to higher frequencies for six members and was fitted to a Rydberg expression in which the quantum defect $\delta = 0.70$. The second Rydberg series, which was also well developed, was calculated to converge on the same series limit (10.88 eV) for a δ of 0.40. The bands in the 1000–2000-Å region and the patterns created by the Rydberg series are shown in Figure 11. The prominent band at 1750 Å, which is the first system encountered in vacuum region, was not placed by Price into a Rydberg scheme, and has been the subject of a number of separate investigations. From a study of the polarized absorption spectra of a number of aliphatic ketones, Barnes and Simpson[87] and Johnson and Simpson[88] established that the polarization of the systems, which corresponded to the 1750-Å transition in formaldehyde, was directed in the molecular plane, perpendicular to the carbonyl bond. With this information and the early SCF calculations, which are given in Table II, Sidman[14] assigned the transition to the promotion of an electron from the nonbonding oxygen orbital to an antibonding σ orbital, namely, $^1B_2(n,\sigma^*) \leftarrow \tilde{X}^1A_1$. That this was a well-founded assignment is attested to by the excellent agreement that Pople and Sidman[59] obtained in their $^1A_2(n,\pi^*) \leftarrow \tilde{X}^1A_1$ intensity borrowing calculations. However, a certain doubt was cast on the foregoing intravalence assignment by the work of Allison and Walsh.[81] Among the bands of H_2CO which were left unassigned by Price[79] and in the spectra of D_2CO, these authors were able to identify a new Rydberg series which converged on the common 10.88-eV limit and was characterized by a δ of 1.04. Moreover under their improved conditions they were able to establish that the series with $\delta = 0.70$ was actually composite and consisted of pairs of bands which could be separately fitted to the Rydberg formulas. The first Rydberg series ($\delta = 1.04$), these authors assigned to electronic transitions which promote an electron from the last filled orbital of the ground-state $b_2n(O)$ to the sets of atom-like orbitals, $a_1 3s$, $a_1 4s$, ... In particular, they assigned the 1750-Å system to the type-b polarized transition, $^1B_2(n,3s) \leftarrow \tilde{X}^1A_1$. The pairs of bands in the second series ($\delta = 0.70$) were assigned to the $b_2n(O) \rightarrow a_1 3p_z$, $a_1 4p_z$, ... and $b_2n(O) \rightarrow b_2 3p_y$, $b_2 4p_y$, ... one-electron promotions which give rise to the type-a and type-b polarized transitions, $^1A_1(n,np_y) \leftarrow \tilde{X}^1A_1$ and $^1B_2(n,np_z) \leftarrow \tilde{X}^1A_1$. The third member of the p Rydberg complex, $^1A_2(n,np_x)$ was not observed since the electric dipole selection rules prevent a combination with the ground state. The third Rydberg series was accounted for as a $b_2n(O) \rightarrow$ 3d, 4d, ... promotion, although Herzberg[89] has felt that the quantum defect of 0.40 is somewhat large for this assignment. The confusion over the orbital assignment of the 1750-Å system which has existed in the literature for some time has been clarified in the elegant *ab initio* calculations of Peyerimhoff, Buenker, Kammer, and Hsu[20] and Whitten and Hackmeyer[19] who placed the $n \rightarrow 3s$ Rydberg at 7.38 and 7.48 eV, respectively. The experimental value which Allison and Walsh[81] obtained for this transition is 7.08 eV. The frequencies of the Rydberg transitions and their assignments are listed in Table XIV. That the 10.88-eV series limit represents the first ionization potential in formaldehyde was aptly demonstrated by Watanabe[90] who measured the ionization threshold from photoionization spectroscopy to be 10.87 eV.

The absorption in the 1750-Å region is dominated by a narrow and intense 0–0 band as would be expected for a transition which involves the electron promotion from a nonbonding orbital to an extravalence orbital which is essentially nonbonding. Information about the upper electronic state, to which this transition is assigned, should come from an analogy to the $^2B_2(n)$ ionic state, to which the $n \rightarrow ns$ Rydberg transitions converge. The photoelectron spectrum of formaldehyde which has recently been obtained by Baker, Baker, Brundle, and Turner[91] is given in Figure 12. The vibrational spectrum of the $^2B_2(n)$ ion appears to be satisfactorily assigned with the vibrational structure accounted for by the activity of all three totally symmetric modes. Their data for the H_2CO/D_2CO fundamentals may be summarized as: $\nu_1 = 2560/1910$, $\nu_2 =$

TABLE XIV. Frequencies[a] (cm^{-1}) of the Observed Rydberg Transitions of H_2CO and D_2CO and Their Isotopic Shifts, $\Delta = \nu_{D_2CO} - \nu_{H_2CO}$

	$^1B_2(n,ns) \leftarrow \tilde{X}^1A_1$			$^1B_2(n,np_z) \leftarrow \tilde{X}^1A_1$		
n	H_2CO	D_2CO	Δ	H_2CO	D_2CO	Δ
3	57,133	57,484	351	64,264	64,472	208
4	74,648	74,821	173	77,643	77,765	122
5	80,807	80,973	166	81,740	81,917	177
6	83,343	83,507	164	83,822	84,013	191
7	84,727	84,881	154	84,952	85,183	231
8	85,545	85,675	130	85,729	85,856	127
9				86,182	86,286	104
	$^1A_1(n,3p_y) \leftarrow \tilde{X}^1A_1$			*n*d series		
3	65,634	65,765	131	71,588	71,678	90
4	77,643	77,765	122	79,359	79,424	65
5				82,727	82,853	126
6				84,349	84,489	140
7				85,377	85,492	115

[a] Data taken from Allison and Walsh.[81]

TABLE XV. Frequencies (cm^{-1}) and Vibrational Assignments of the Observed Bands[a] of the $^1B_2(n,3s) \leftarrow \tilde{X}^1A_1$ and $^1A_1(n,3p_y) \leftarrow \tilde{X}^1A_1$ Rydberg Transitions

Assignment	H_2CO	Δν	D_2CO	Δν
		$^1B_2(n,3s) \leftarrow \tilde{X}^1A_1$		
3_1^0			56,387	−1104
0–0	57,180	0	57,419	0
	57,526	346		
	58,002	822	57,992	501
2_0^1	58,757	1577	58,774	p1283
1_0^1	59,455	2275	59,192	1701
1_0^2	61,430	4250	60,840	3349
		$^1A_1(n,3p_y) \leftarrow \tilde{X}^1A_1$		
$3_1^0(P)$			63,342	−1103
$3_1^0(R)$			63,396	
$3_1^1(P)$			64,110	347
$3_1^1(R)$			64,155	
0–0(P)	64,243		64,448	0
0–0(R)	64,309		64,498	
$3_0^1(P)$			65,205	757
$3_0^1(R)$			65,256	

[a] Data taken from Moule and Bell.[92]

1590/1560, ν_3 = 1210/870. Moule and Bell[92] have recently made a study of the vacuum ultraviolet spectrum of formaldehyde under improved conditions of resolution. Figure 13 illustrates the spectra of H_2CO and D_2CO which were recorded over the 1500–1800-Å region with a 3-m McPherson spectrograph at a dispersion of 2.7 Å/mm. Table XV lists the wave numbers of some of the bands in this region, along with their assignments. The assignment of the bands at higher frequencies is relatively straightforward. From a correlation to the 2560-cm^{-1} frequency of the $^2B_2(n)$ ion, the +2275 and +4250 bands of H_2CO are assigned to the fundamental and first overtones of the CH stretching modes, 1_0^1 and 1_0^2. The corresponding values of +1701 and +3350 cm^{-1} in D_2CO display the correct isotope shift to be given the same assignment. The band at +1577 cm^{-1} in H_2CO correlates well with the 1590-cm^{-1} band and is assigned as 2_0^1. The assignment of this region in the D_2CO spectrum does present some difficulties as the only available band is at +1283 cm^{-1}. If this assignment were correct it would be necessary to invoke a Fermi resonance between ν_2' and perhaps $2\nu_3'$ to explain the effect. For an exact resonance, this would give ν_3' a value of 775 cm^{-1}

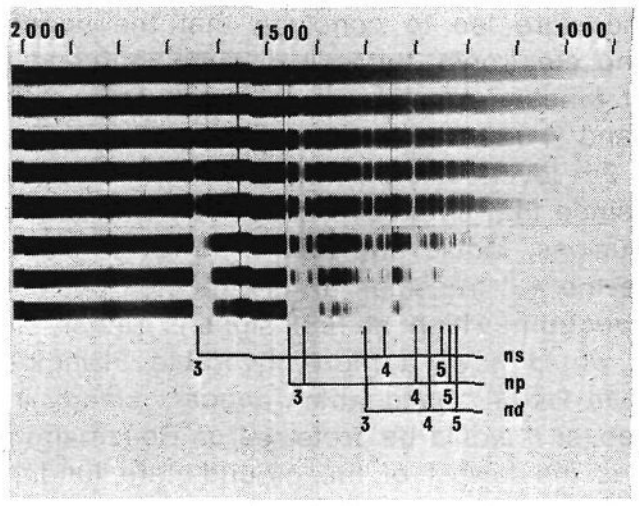

Figure 11. The absorption spectrum of H_2CO from 2000 to 1000 Å (after Allison and Walsh, ref 81).

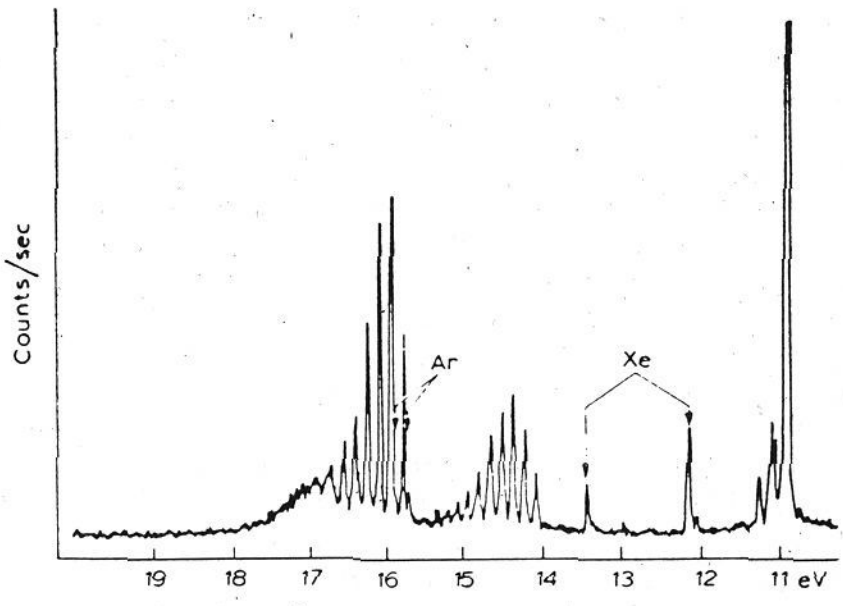

Figure 12. The photoelectron spectrum of H_2CO (Baker, Baker, Brundle, and Turner, ref 91).

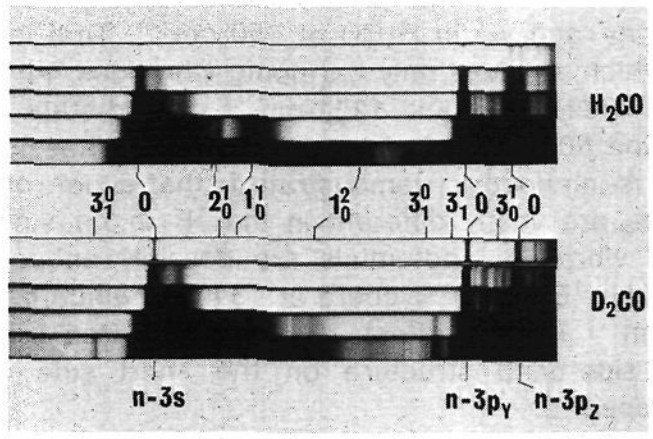

Figure 13. Absorption spectra of H_2CO and D_2CO from 1500 to 1800 Å recorded with a 3-m McPherson spectrograph (Moule and Bell, ref 92).

which is very similar to the ν_3' = 757 cm^{-1} which has been observed for the $^1A_1(n,3p_y)$ state. The hot band in the D_2CO spectrum which appears clearly at −1104 cm^{-1} may be assigned as 3_1^0 as the infrared data gives ν_3'' = 1106 cm^{-1}. The strength of this band, which bears a Boltzmann factor of 4.5 × 10^{-3}, attests to the activity of ν_3' in the spectrum, which through a straightforward Franck–Condon argument would be the result of a significant change in the HCH angle on excitation.

The most prominent of the vibronic features which are associated with the 0–0 band in H_2CO are a pair of diffuse shoulders at +346 and +822 cm^{-1}. In D_2CO diffuse structure appears at 501 cm^{-1}. (It may, of course, be that 501 cm^{-1} in D_2CO corresponds to the 822-cm^{-1} shoulder in H_2CO, and that the 346-cm^{-1} analog of H_2CO has become fused with the 0–0 band of H_2CO.) The origin of these bands has been the object of some speculation. Allison and Walsh[81] considered the intervals to be too small to be accounted for by harmonic vibra-

tions and were led to conclude that the upper of the combining electronic states was nonplanar and that the potential function for ν_4' was strongly anharmonic. The +346- and +822-cm^{-1} intervals were assigned to the 1+ and 2+ levels of the ν_4 inversion manifold. All of the studies since that time have concurred with these general conclusions. Moule and Bell,[92] however, were unable to locate the 4_1^1 transition at its expected position in the D_2CO spectrum which at first sight is rather surprising since it would have a more favorable Franck–Condon factor than the 3_1^0 band which appears clearly in Figure 13. Moreover it would be preferred on Boltzmann grounds since it is the lowest of the ground-state fundamentals. Predissociation effects in the ν_4 manifold of levels, which are clearly evident in H_2CO, could occur in D_2CO to the extent that the 4_1^1 transition would be too broadened to be observed against the diffuse background of the 0–0 transition. The $\nu(D_2CO)-\nu(H_2CO)$ isotope shifts given in Table XIV do illustrate that the vibrational frequencies are very different in the $^1B_2(n,3s)$ state from what they are in the higher Rydberg transitions. Indeed the isotope shift for the $n \rightarrow 3s$ transition is three times larger than the shift of the $n \rightarrow \pi^*$ transition; *viz.*, 351 and 113 cm^{-1}. It is possible to obtain a rough idea of the changes in vibrational frequency, $\Delta\nu$, on electronic excitation by assuming that the vibrations in the two states are harmonic and then summing the zero-point energies over the six normal modes of H_2CO and D_2CO. If the assumptions are made: (i) that 3_0^1 is correctly assigned in the D_2CO spectrum, (ii) that the isotope ratios $\nu(H_2CO)/\nu(D_2CO)$ are identical in the $\tilde{X}^1A_1$ and $^1B_2(n,3s)$ states, (iii) that ν_1' and ν_5', the symmetric and antisymmetric C–H vibrations, suffer the same frequency shifts on excitation, the calculation shows that the 351-cm^{-1} origin isotope shift is only compatible with an average downward frequency shift, $\Delta\nu$, for both ν_4' and ν_6' in H_2CO of 750 cm^{-1}. That is, for a model which employs only harmonic vibrations, ν_4 and ν_6 fall from their 1167- and 1251-cm^{-1} ground-state values to 417 and 501 cm^{-1} in the excited state. What this calculation is intended to demonstrate is that either, or both, ν_4 and ν_6 are vastly different in the $^1B_2(n,3s)$ state and that the vibrational potentials are possibly anharmonic. Indeed, the $^1B_2(n,4s)$ Rydberg at 1340 Å, which has only a 173-cm^{-1} isotope effect, is completely free from the rippling side-band structure on the short side of the 1750-Å spectra.

The precise assignment of the Rydberg doublet which appears in the 1525-Å region was made from *ab initio* calculations of Peyerimhoff, Buenker, Kammer, and Hsu[20] who showed that the 7.97-eV system (1556 Å) was to be associated with the $^1A_1(n,3p_y) \leftarrow \tilde{X}^1A_1$ transition, and the 8.14-eV system (1526 Å) with the $^1B_2(n,3p_z) \leftarrow \tilde{X}^1A_1$ transition. Mentall, Gentieu, Krauss, and Neumann[22] observed that the 0–0 band at the 1556-Å system was doubled, which led them to assign the individual components to a pair of transitions which terminated on the 0+ and 0− members of a ν_4 inversion doublet. A close inspection of Figure 13 reveals, however, that a number of bands in the D_2CO spectrum are doublets and are characterized by a constant splitting of 50 cm^{-1}. The electronic transition shows the correct vibrational activity of a nonbonded to Rydberg-orbital transition, and it is to be inferred, on Franck–Condon grounds, that the structural changes on electronic excitation are quite small. The rotational envelopes of the 0–0 and ν_1', ν_2', and ν_3' bands should resemble those of a type-a infrared band. The spectrum obtained by Ebers and Nielsen[34] shows that there is indeed a one-to-one correlation between the P and R wings of the 1700-cm^{-1} ν_2'' infrared band of D_2CO and the envelope of the 1526-Å doublet. In the D_2CO spectrum the bands at +757, −347, and −1103 cm^{-1} can be nicely fitted into a pattern involving the quanta of ν_3; *viz.*, 3_0^1, 3_1^1, and 3_1^0, which places ν_3' at 757 cm^{-1}. This value is to be compared with the 775-cm^{-1} interval of the $^1B_2(n,3s)$ state.

The vibrational structure of the 1526-Å system is complex and contains many features which have yet to be assigned. As Figure 13 illustrates, the bands at 1526 and 1521 Å in H_2CO coalesce into a single peak in the D_2CO spectrum. This behavior vitiates the assignment of Mentall, Gentieu, Krauss, and Neumann[22] who ascribed these peaks to transitions which terminate on the 0+ and 1+ inversion levels. Assignable structure does appear at +1066 in H_2CO and at 828 cm^{-1} in D_2CO which because of the magnitude and ratio of these intervals can be given the designation 3_0^1.

Only recently has an attempt been made to locate and assign the Rydberg series which lie beyond the first ionization potential in formaldehyde. Using a windowless differential-pumping technique, Mentall, Gentieu, Krauss, and Neumann[22] have been able to extend the absorption spectroscopy of H_2CO down to 600 Å. Their results have recently been supplemented by the inelastic electron scattering spectrum of Weiss, Kuyatt, and Mielczarek,[86] which is illustrated in Figure 14. It should be possible to get an idea of what transitions to expect in the 11–16-eV region by subtracting an estimated value of th *ns*, *np*, and *nd* Rydberg terms from the higher ionization limits which are known from photoelectron spectroscopy. The second system in the photoelectron spectrum of H_2CO which sets in at 14.09 eV has been assigned to a $^2B_1(\pi) \leftarrow \tilde{X}^1A_1$ transition by Baker, Baker, Brundle, and Turner[91] and consists of a single progression of bands with a spacing of 0.150 eV (1210 cm^{-1}). This information, coupled with the single-configuration SCF calculations of Mentall, *et al.*,[22] who demonstrated that the term values of the $^2B_1(\pi)$ ion are similar to the $^2B_2(n)$ ion allows one to predict that the $^1B_1(\pi,3s) \leftarrow \tilde{X}^1A_1$, and $^1B_1(\pi,3p_z) \leftarrow \tilde{X}^1A_1$ transitions should lie at 10.29 and 11.16 eV. The electron scattering as well as the absorption measurements show that the region beyond the first ionization limit and up to 12.5 eV is surprisingly free from bands which indicates that the s-, p-, and d-type series resulting from the excitation of a π electron are not formed. Moule and Bell[92] have observed a peculiar band in the spectra of H_2CO, HDCO, and D_2CO which is illustrated in Figure 15 at 1235 Å (10.1 eV) which does not fit into the scheme of the first Rydberg transitions. The observed value for this band compares favorably with the value predicted for the $^1B_1(\pi,3s) \leftarrow \tilde{X}^1A_1$ transition. The major difficulty with the assignment, though, is that the expected 2_0^1, 2_0^2 members of the ν_2' carbonyl stretching frequency are not observed. From a study of the mass-analyzed photoionization spectrum, Guyon and Chupka[93] have observed a series leading to a $^2B_1$ limit with an effective quantum defect of 0.1.

The strong band with a maximum at 13.13 eV (945 Å) which is observed in both absorption and electron scattering spectra is probably composed of both an s- and p-type series converging to the third ionization potential of H_2CO. As suggested by the photoelectron spectra of the third electronic band system of H_2CO^+, one would expect the $n\sigma \rightarrow ns,np, \ldots$ Rydberg transitions to be excited predominantly in the ν_2 mode. The 13.13-eV peak has been tentatively assigned by Weiss, Kuyatt, and Mielczarek[86] as the first member of the $n\sigma \rightarrow np$ Rydberg transitions converging to the 15.85-eV limit with a quantum defect of roughly 0.8 eV.

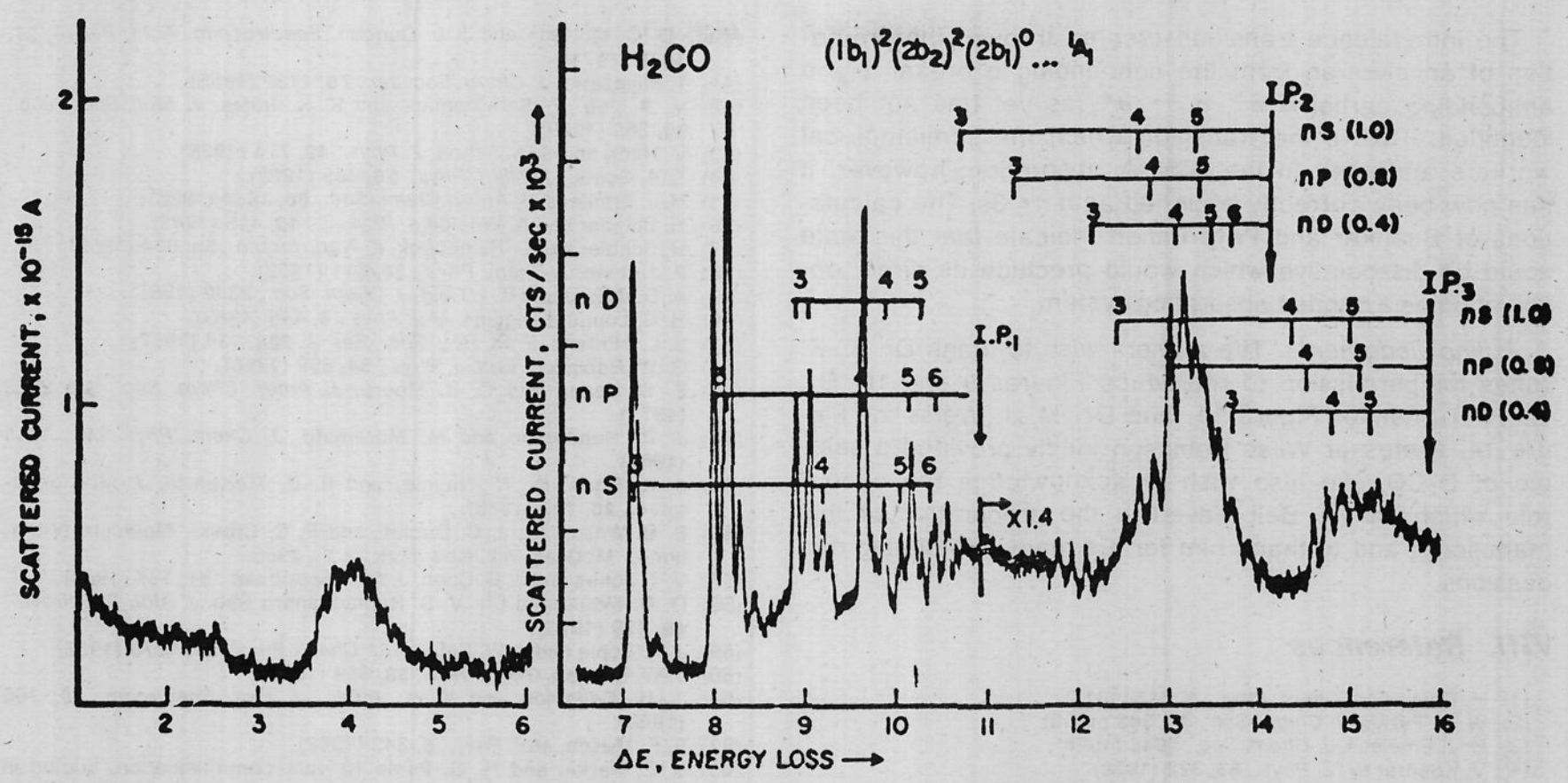

Figure 14. Inelastic electron scattering spectrum of H_2CO (Weiss, Kuyatt, and Mielczarek, ref 86).

VII. $^1B_1(n\sigma,\pi^*)$, $^1A_1(\pi,\pi^*)$, and $^1B_2(n,\sigma^*)$ States

While the low-energy $^1A_2(n,\pi^*)$ state seems to be satisfactorily accounted for from an experimental as well as a theoretical point of view, the picture for the higher intravalence states is not so clear. We consider first the $^1B_1(n\sigma,\pi^*)$ state since our knowledge here is better than it is of the other remaining intravalence states. In the one-electron MO picture, the $^1B_1(n\sigma,\pi^*) \leftarrow \tilde{X}^1A_1$ transition is depicted as an electron transfer from a bonding σ orbital (second nonbonding oxygen orbital) to the carbonyl π^* orbital. The presence of the partially filled π^* orbital would then have the effect of lengthening the CO bond as well as creating a structural instability in the out-of-plane direction. These expectations have been theoretically confirmed in the SCF–CI calculations of Buenker and Peyerimhoff[18] which are given in Table III. The results of the semiempirical and *ab initio* MO calculations of Table II, which compare the vertical electronic transition energies, show that the transition should fall in the 8.4–9.4-eV range. The H_2CO absorption spectrum of Allison and Walsh, Figure 11, does display a banded region in the 1370–1440-Å region, which Mentall, Gentieu, Krauss, and Neumann[22] assign to the *x*-polarized $^1B_1(n\sigma,\pi^*) \leftarrow \tilde{X}^1A_1$ transition. They attribute the observed irregular 157- and 487-cm^{-1} band intervals to the activity of the carbonyl stretching frequency, although these intervals appear to be very small when a comparison is made to the 1746-cm^{-1} ground-state value.

The whereabouts of the $^1A_1(\pi,\pi^*) \leftarrow \tilde{X}^1A_1$ transition has been a source of considerable speculation. Since the normal self-consistent procedures cannot be applied to the π,π^* electron configuration, the theoretical estimates of the vertical transition energies have been at variance. The most extensive of these calculations are those of Whitten[21] who expanded his basis set to include d_{xz} orbitals as well as a CI mixing of $\sigma\sigma^*$ excitations. His value of 9.9 eV for the vertical transition energy should be regarded as the most reliable of those listed in Table II. Both Whitten[21] and Buenker and Peyerimhoff[18] find that the potential surface of the π,π^* state is dissociative with respect to carbonyl bond stretching which is not too surprising since the CO double bond is effectively broken on

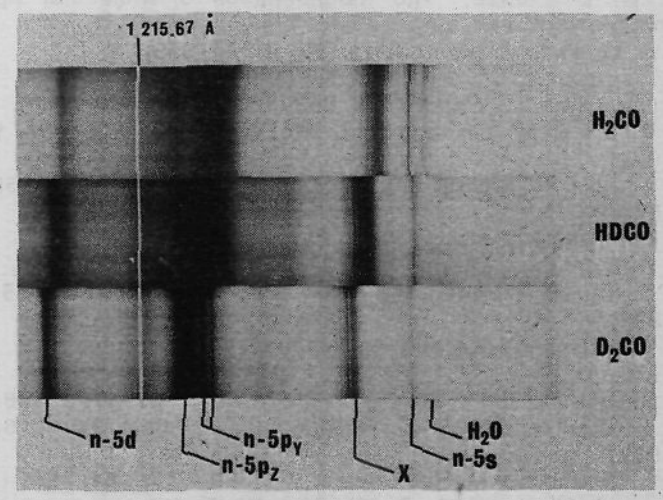

Figure 15. Absorption spectra of H_2CO, HDCO, and D_2CO in the 1240-Å region, recorded with 3-m McPherson spectrograph (*Moule and Bell, ref 92*).

$\pi \rightarrow \pi^*$ excitation. No experimental evidence for the $^1A_1(\pi,\pi^*) \leftarrow \tilde{X}^1A_1$ transition can be found in either the absorption or the electron scattering spectra which is one of central puzzles of the spectroscopy of this region. Mentall, Gentieu, Krauss, and Neumann[22] suggest that the absence of structure could be attributed to a Rydberg-valence mixing. They performed model calculations to take account of the interaction of the π,π^* intravalence configuration with the $n \rightarrow ns$, np, nd, and $\pi \rightarrow ns$, np, nd series and found, in particular that one Rydberg state, the $^1A_1$ (n, 3d) state, was interacting to the extent that it contained 30% of the character of the π,π^* configuration. This would explain the erratic behavior of the 0.4 quantum defects observed for the $n \rightarrow nd$ Rydberg series. Mentall, *et al.*, also suggest that the π,π^* configuration could be autoionized in the limiting continuum of the $n \rightarrow nd$ Rydberg series and thereby lose its vibrational fine structure. The explanation of Whitten seems equally likely; namely, that the π,π^* state is dissociative in the CO direction and that transitions from the ground state give rise to an extensive absorption continuum. The π,π^* state may be perturbing the $^2B_1(\pi^*)$ Rydberg series as well, which could explain the absence of the first members of this series. Perturbation effects could also extend into the band at 12 to 14 eV as the experimental oscillator strength of 1.12 here is unusually large.

The intravalence transition created through the promotion of an electron from the nonbonding n orbital to the antibonding carbonyl σ^*, n $\rightarrow$ σ^*, as yet has not been identified. This is the transition which the semiempirical workers attributed to the 1750-Å absorption; however, it has now been correctly assigned as n $\rightarrow$ 3s. The calculations of Buenker and Peyerimhoff indicate that this state could be dissociative which would preclude its direct observation as a banded absorption system.

Acknowledgments. The authors wish to thank Dr. K. K. Innes for permission to reproduce Figures 9 and 10, Dr. D. W. Turner for Figure 11, and Dr. M. J. Weiss for Figure 14. Professor Wilse Robinson kindly provided a sample of D_2CO. We also wish to acknowledge the central role which Dr. S. Bell played in the preparation of this manuscript and to thank him for his many stimulating discussions.

VIII. References

(1) H. Davy, *Ann. Chem. Phys.*, **4**, 347 (1817).
(2) W. H. Perkin, *J. Chem. Soc.*, 41, 363 (1882).
(3) H. J. Emeléus, *J. Chem. Soc.*, 2948 (1926).
(4) V. Kondrat'ev, *Z. Phys.*, **63**, 322 (1930).
(5) G. Herzberg and K. Franz, *Z. Phys.*, **76**, 720 (1932).
(6) S. Gradstein, *Z. Phys. Chem. B*, **22**, 384 (1933).
(7) R. W. B. Pearse, "The Indentification of Molecular Spectra," Chapman and Hall, Ltd., London, 1941.
(8) R. S. Mulliken, *J. Chem. Phys.*, **23**, 1997 (1955).
(9) A. D. Walsh, *J. Chem. Soc.*, 2306 (1953).
(10) J. C. D. Brand, *J. Chem. Soc.*, 858 (1956).
(11) I. Absar, C. S. Lin, and K. L. McEwen, *Can. J. Chem.*, **50**, 646 (1972).
(12) R. L. Ellis, R. Squire, and H. H. Jaffé, *J. Chem. Phys.*, **55**, 3500 (1971).
(13) T. Anno and A. Sado, *J. Chem. Phys.*, **26**, 1759 (1957).
(14) J. W. Sidman, *J. Chem. Phys.*, **27**, 429 (1957).
(15) J. C. Ho, G. A. Segal, and H. S. Taylor, *J. Chem. Phys.*, **56**, 1520 (1972).
(16) C. Giessner-Prettre and A. Pullman, *Theor. Chim. Acta*, **18**, 14 (1970).
(17) T. H. Dunning and V. McKoy, *J. Chem. Phys.*, **47**, 1735 (1967).
(18) R. J. Buenker and S. D. Peyerimhoff, *J. Chem. Phys.*, **53**, 1368 (1970).
(19) J. L. Whitten and M. Hackmeyer, *J. Chem. Phys.*, **51**, 5584 (1969).
(20) S. D. Peyerimhoff, R. J. Buenker, W. E. Kammer, and H. Hsu, *Chem. Phys. Lett.*, **8**, 129 (1971).
(21) J. L. Whitten, *J. Chem. Phys.*, **56**, 5458 (1972).
(22) J. E. Mentall, E. P. Gentieu, M. Krauss, and D. Neumann, *J. Chem. Phys.*, **55**, 5471 (1971).
(23) H. L. McMurray and R. S. Mulliken, *Proc. Nat. Acad. Sci. U.S.*, **26**, 312 (1940).
(24) R. N. Dixon, *Mol. Phys.*, **12**, 83 (1967).
(25) H. W. Kroto and P. D. Santry, *J. Chem. Phys.*, 47, 2736 (1967).
(26) D. A. Condirston and D. C. Moule, *Theor. Chim. Acta*, **29**, 133 (1973).
(27) G. H. Dieke and G. B. Kistiakowsky, *Phys. Rev.*, **45**, 4 (1934).
(28) G. Herzberg, "Infrared and Raman Spectra," Van Nostrand, New York, N.Y., 1949.
(29) D. W. Davidson, B. I. Stoicheff, and H. J. Bernstein, *J. Chem. Phys.*, **22**, 289 (1954).
(30) D. B. Stevenson, J. E. LuValle, and V. Schomaker, *J. Amer. Chem. Soc.*, **61**, 2508 (1939).
(31) D. R. Johnson, F. J. Lovas, and W. H. Kirchoff, *J. Phys. Chem. Ref. Data*, 1, No. 4 (1972).
(31a) T. Oka, H. Kirakawa, and K. Shimoda, *J. Phys. Soc. Jap.*, **15**, 2265 (1960).
(31b) L. Esterowitz, *J. Chem. Phys.*, **39**, 247 (1963).
(31c) T. Ika, K. Takagi, and Y. Morino, *J. Mol. Spectrosc.*, **14**, 27 (1964).
(31d) H. Takuma, K. M. Evenson, and T. Shigenari, *J. Phys. Soc. Jap.*, **21**, 1622 (1966).
(31e) M. Takami, *J. Phys. Soc. Jap.*, **24**, 372 (1968).
(31f) K. D. Tucker, G. R. Tomasevich, and P. Thaddeus, *Astrophys. J.*, **161**, L153 (1970).
(31g) K. D. Tucker, G. R. Tomasevich, and P. Thaddeus, *Astrophys. J.*, **169**, 429 (1971).
(32) K. Takagi and T. Oka, *J. Phys. Soc. Jap.*, **18**, 1174 (1963).
(33) E. S. Ebers and H. H. Nielsen, *J. Chem. Phys.*, **5**, 822 (1937).
(34) E. S. Ebers and H. H. Nielsen, *J. Chem. Phys.*, **6**, 311 (1938).
(35) H. H. Blau, Jr., and H. H. Neilsen, *J. Mol. Spectrosc.*, 1, 124 (1957).
(36) J. R. Patty and H. H. Nielsen, *Phys. Rev.*, **39**, 957 (1932).
(37) H. H. Nielsen, *Phys. Rev.*, **46**, 117 (1934).
(38) T. Nakagawa, H. Kashiwagi, H. Kurihara, and Y. Morino, *J. Mol. Spectrosc.*, **31**, 436 (1969).
(39) I. C. Hisatsune and D. F. Eggers Jr., *J. Chem. Phys.*, **23**, 487 (1955).
(40) E. C. Curtis, *J. Mol. Spectrosc.*, **14**, 279 (1964).
(40a) T. Oka and Y. Morino, *J. Phys. Soc. Jap.*, **16**, 1235 (1961).
(40b) T. Shimanouchi and I. Suzuki, *J. Chem. Phys.*, **42**, 296 (1965).
(40c) D. C. McKean and J. L. Duncan, *Spectrochim. Acta, Part A*, **27**, 1879 (1971).
(41) T. Miyazawa, *J. Chem. Soc. Jap.*, **76**, 1132 (1955).
(42) V. A. Job, V. Sethuraman, and K. K. Innes, *J. Mol. Spectrosc.*, **30**, 365 (1969).
(43) V. Henri and S. A. Schou, *Z. Phys.*, **49**, 774 (1928).
(44) S. A. Schou, *J. Chim. Phys.*, **26**, 665 (1929).
(45) H. J. Emeléus, *J. Amer. Chem. Soc.*, **60**, 1864 (1938).
(46) H. Schuler and A. Woeldike, *Phys. Z.*, **43**, 415 (1942).
(47) H. Schuler and L. Reinebeck, *Z. Naturforsch.*, **5a**, 604 (1950).
(48) P. J. Dyne, *J. Chem. Phys.*, **20**, 811 (1952).
(49) A. D. Cohen and R. I. Reid, *J. Chem. Soc.*, 2386 (1957).
(50) H. C. Longuet-Higgins, *Mol. Phys.*, **6**, 445 (1963).
(51) S. L. Altmann, *Proc. Roy. Soc., Ser. A*, **298**, 184 (1967).
(52) G. W. Robinson, *Can. J. Phys.*, **34**, 699 (1956).
(53) E. S. Yeung and C. B. Moore, *J. Amer. Chem. Soc.*, **93**, 2059 (1971).
(54) J. R. Henderson and M. Muramoto, *J. Chem. Phys.*, **43**, 1215 (1965).
(55) J. B. Coon, N. W. Naugle, and R. D. McKenzie, *J. Mol. Spectrosc.*, **20**, 107 (1966).
(56) E. B. Wilson Jr., J. C. Decius, and P. C. Cross, "Molecular Vibrations," McGraw-Hill, New York, N.Y., 1955.
(57) V. T. Jones and J. B. Coon, *J. Mol. Spectrosc.*, **31**, 137 (1969).
(58) D. C. Moule and Ch. V. S. Ramachandra Rao, *J. Mol. Spectrosc.*, **45**, 120 (1973).
(59) J. A. Pople and J. W. Sidman, *J. Chem. Phys.*, **27**, 1270 (1957).
(60) J. W. Sidman, *Chem. Rev.*, **58**, 689 (1958).
(61) J. H. Callomon and K. K. Innes, *J. Mol. Spectrosc.*, **10**, 166 (1963).
(62) S. F. Mason, *Mol. Phys.*, **5**, 343 (1962).
(63) J. E. Parkin and H. G. Poole (private communication, quoted in ref 61).
(64) J. C. D. Brand, J. H. Callomon, and J. K. G. Watson, *Discuss. Faraday Soc.*, **35**, 175 (1963).
(65) V. Sethuraman, V. A. Job, and K. K. Innes, *J. Mol. Spectrosc.*, **33**, 189 (1970).
(66) G. W. Robinson and V. E. DiGiorgio, *Can. J. Chem.*, **36**, 31 (1958).
(67) W. T. Raynes, *J. Chem. Phys.*, **44**, 2755 (1966).
(68) D. S. McClure, *J. Chem. Phys.*, **20**, 682 (1952).
(69) J. W. Sidman, *J. Chem. Phys.*, **29**, 644 (1958).
(70) H. F. Hameka and L. J. Oosterhoff, *Mol. Phys.*, 1, 358 (1958).
(71) M. A. El-Sayed, *J. Chem. Phys.*, **41**, 2462 (1964).
(72) D. G. Carroll, L. G. Van Quickenborne, and S. P. McGlynn, *J. Chem. Phys.*, **45**, 2777 (1966).
(73) T. Yonezawa, H. Kato, and M. Kato, *J. Mol. Spectrosc.*, **24**, 500 (1967).
(74) V. E. DiGiorgio and G. W. Robinson, *J. Chem. Phys.*, **31**, 1678 (1959).
(75) A. B. F. Duncan and E. H. House, as quoted by J. W. Sidman, ref 66.
(76) S. E. Hodges, J. R. Henderson, and J. B. Coon, *J. Mol. Spectrosc.*, **2**, 99 (1958).
(77) F. W. Birss, R. Y. Dong, and D. A. Ramsay, *Chem. Phys. Lett.*, **18**, 11 (1973).
(78) J. T. Hougen, *J. Chem. Phys.*, **41**, 363 (1964).
(79) W. C. Price, *J. Chem. Phys.*, **3**, 256 (1935).
(80) G. Fleming, M. M. Anderson, A. J. Harrison, and L. W. Pickett, *J. Chem. Phys.*, **30**, 351 (1959).
(81) K. Allison and A. D. Walsh, Chemical Institute of Canada Symposium, Ottawa, 1957.
(82) S. Bell, Thesis, University of Dundee, 1961.
(83) L. E. Snyder, D. Buhl, B. Zuckerman, and P. Palmer, *Phys. Rev. Lett.*, **22**, 679 (1969).
(84) E. P. Gentieu and J. E. Mentall, *Science*, **169**, 681 (1970).
(85) J. E. Mentall, E. P. Gentieu, M. Krauss, and D. Neumann, *J. Chem. Phys.*, **55**, 5471 (1971).
(86) M. J. Weiss, C. E. Kuyatt, and S. Mielczarek, *J. Chem. Phys.*, **54**, 4147 (1971).
(87) E. E. Barnes and W. T. Simpson, *J. Chem. Phys.*, **39**, 670 (1963).
(88) W. C. Johnson, Jr., and W. T. Simpson, *J. Chem. Phys.*, **48**, 2168 (1968).
(89) G. Herzberg, "Electronic Spectra of Polyatomic Molecules," Van Nostrand, New York, N.Y., 1966.
(90) K. Watanabe, *J. Chem. Phys.*, **26**, 542 (1957).
(91) A. D. Baker, C. Baker, C. R. Brundle, and D. W. Turner, *Int. J. Mass Spectrosc. Ion Phys.*, 1, 285 (1968).
(92) D. C. Moule and S. Bell, unpublished results.
(93) P. Guyon and W. A. Chupka, as quoted by ref 22.
(94) D. E. Freeman and W. Klemperer, *J. Chem. Phys.*, **40**, 604 (1964).
(95) D. E. Freeman and W. Klemperer, *J. Chem. Phys.*, **45**, 52 (1966).
(96) K. Kondo and T. Oka, *J. Phys. Soc. Jap.*, **15**, 307 (1960).
(97) J. R. Lombardi, D. E. Freeman, and W. Klemperer, *J. Chem. Phys.*, **46**, 2746 (1967).
(98) N. J. Bridge, D. A. Haner, and D. A. Dows, *J. Chem. Phys.*, **48**, 4197 (1968).
(99) N. J. Bridge, D. A. Haner, and D. A. Dows, *J. Chem. Phys.*, **44**, 3128 (1966).
(100) A. D. Buckingham and D. A. Ramsay, *J. Chem. Phys.*, **42**, 3721 (1965).
(101) P. Kusch and F. W. Loomis, *Phys. Rev.*, **55**, 850 (1939).
(102) W. H. Eberhardt and H. Renner, *J. Mol. Spectrosc.*, **6**, 483 (1961).
(103) J. E. Parkin, H. G. Poole, and W. T. Raynes, *Proc. Chem. Soc., London*, 248 (1962).
(104) J. C. D. Brand and C. G. Stevens, *J. Chem. Phys.*, **58**, 3331 (1973).